AD

USAAVLABS TECHNICAL REPORT 65-76

A PRELIMINARY STUDY TO DETERMINE THE FEASIBILITY OF REINFORCED PLASTIC COLUMN MEMBERS FOR AIRCRAFT STRUCTURES

By

Dev R. Bhandari

December 1965

U. S. ARMY AVIATION MATERIEL LABORATORIES
FORT EUSTIS, VIRGINIA

CONTRACT DA 44-177-AMC-892(T)
THE AEROPHYSICS DEPARTMENT
MISSISSIPPI STATE UNIVERSITY
STATE COLLEGE, MISSISSIPPI

DEPARTMENT OF THE ARMY
U. S. ARMY AVIATION MATERIEL LABORATORIES
FORT EUSTIS, VIRGINIA 23604

This experiment was conducted in connection with the Marvel program. It has been reviewed by the U. S. Army Aviation Materiel Laboratories and is considered to be technically sound. The report is published for the exchange of information and the stimulation of ideas.

Task 1P125901A14203
Contract DA 44-177-AMC-892(T)
USAAVLABS Technical Report 65-76
December 1965

A PRELIMINARY STUDY TO DETERMINE THE FEASIBILITY OF REINFORCED PLASTIC COLUMN MEMBERS FOR AIRCRAFT STRUCTURES

Aerophysics Research Report No. 60

by

Dev R. Bhandari

Prepared by

The Aerophysics Department
Mississippi State University
State College, Mississippi

for

U. S. ARMY AVIATION MATERIEL LABORATORIES
FORT EUSTIS, VIRGINIA

ABSTRACT

Empirical formulas for predicting the critical buckling stress of fiber glass reinforced plastic columns have been obtained. On the basis of these buckling formulas, structural efficiency of fiber glass reinforced plastic column members of different cross sections is compared with other commonly used structural alloys. The efficiency parameter used for comparison is derived on the minimum weight design considerations.

CONTENTS

TABLES

ILLUSTRATIONS

SYMBOLS

A	Area of cross section, in^2
b	Semi-width of cross section, in
C	Restraint coefficient for columns
D	Diameter of tube, in
ϵ	Deflection per inch of test specimens, in/in
E	Modulus of elasticity (Young's modulus), lb/in^2
E_r	Reduced modulus of elasticity, lb/in^2
$\bar{E}$	Effective modulus of elasticity, lb/in^2
Ea	Apparent modulus of elasticity, lb/in^2
F	Compressive stress, lb/in^2
F_m	Maximum stress of a ¼-inch thick laminate under compression lb/in^2
h	Semi-depth of cross section, in
I	Moment of inertia, in^4
K_1	Nondimensional coefficient in local buckling formula for flat plate
K_2	Nondimensional coefficient in local buckling formula for circular plate
k_1	Factor for shape parameter
k/Fm	Compressive or tensile strength reduction factor
k/Em	Compressive or tensile modulus reduction factor
L	Column length, in
m	Ratio h/b
psi	Pounds per in^2
P	Applied load, lb

P_{cr}	Critical load, lb
R	Radius, in
t	Thickness, in
w	Density, lb/in^3
W	Weight, lb
ℓ	Radius of gyration ($= \sqrt{I/A}$), in
L/ℓ	Slenderness ratio
P/L^2	Structural index, lb/in^2
η	Column efficiency
δ	Deflection, in
σ_{max}	Maximum compressive stress, lb/in^2
σ_{co}	Euler buckling stress, lb/in^2
σ_{ccr}	Local buckling stress, lb/in^2
σ	Axial stress, lb/in^2
τ	Reduced modulus ratio ($= E_r/E$)
θ	Angle between the direction of applied load and the primary direction of the fabric (the warp and weft)

INTRODUCTION

One of the main considerations for an aircraft designer is saving as much structural weight as possible, which means an increase in payload, better performance and possibly less running cost. To achieve this objective, researchers have been working to find better materials and to develop improved and more efficient methods of design.

Aircraft designers during the past few years have been using fiber glass reinforced plastics for nonstructural parts of aircraft. Recently, fiber reinforced materials, especially fiber glass reinforced plastic laminates, have shown great potential for use as primary structural components in aeronautical design.

Many research publications (references 2-4, 6, 15, 19, 20-22, and 24) are made available by the U. S. Forest Products Laboratory and other research organizations which give physical and mechanical properties for all types of fiber glass reinforced plastic laminates. The principal advantage of fiber glass reinforced plastic is its extremely high strength-to-weight ratio which is superior to that of other structural materials. In addition, fiber glass reinforced plastics possess other excellent properties; viz., resistance to chemical corrosive environments, simple and easy techniques in fabricating complex structural parts, easy handling, low cost of tooling, high-impact resistance and numerous other properties.

These qualities, along with the recent advances in processing techniques and the development of high-temperature-resistant laminates, have caused aircraft designers to become interested in using structures made from fiber glass reinforced plastic materials. It is possible that the availability of such materials will revolutionize the design developments in the aeronautical field.

A large amount of published data on optimum design techniques (references 5, 7, 8, and 23) is available for different types of loadings. Compression of thin-walled closed and open sections and torsion of thin-walled cells are problems which are of interest to aircraft, marine and civil engineers.

In 1943 Cox and Smith published a systematic analysis of compression members. They introduced the concept of a structural loading of coefficient which is generally the ratio of the compression load P to the square of the dimension L. They showed that for the same material of construction the minimum weight depends upon the structural loading coefficient.

The same approach was used by Shanley (reference 13) and was later dealt with more comprehensively in a book (reference 14) by the same

author. The author points out that the structures of maximum structural efficiency are designed on the basis of simultaneous failure occurring in all critical modes. When a thin-walled compression member is subjected to an axial thrust, generally there can be three modes of failure: (1) primary or Euler buckling, (2) secondary or local buckling, and (3) material failure. Any combination of these may also take place.

The structural loading coefficient or the structural index (P/L^2) can be used as a basis for comparing the structural efficiency of various materials.

The main purpose of this report is to determine the feasibility of using reinforced plastic column members in aircraft structures by design studies and the fabrication and testing of the column specimens. This study is not possible unless column buckling formulas for reinforced plastics are available.

The work in these investigations has been directed first toward finding the empirical formulas for predicting the critical buckling stress of fiber glass reinforced plastic column members and, secondly, toward investigating whether reinforced plastics provide structures efficient on a strength-to-weight basis when compared with other commonly used structural alloys.

To obtain the column buckling formulas for fiber glass reinforced plastics, compression tests on 24 column members of circular cross section in 10 different lengths were carried out. Then column members of different cross sections designed on the basis of simultaneous failures were analyzed and an efficiency parameter was derived which provided a basis for comparing the column efficiency of different materials.

MATERIALS

Numerous publications giving the compositions of all types of inorganic fibers - glass, ceramic, refractory, asbestos and metal - are available. Presenting the metallurgy of all fibers would be a task beyond the scope of this report, but an extensive list of references is given in a research report by R. H. Baskey (reference 1).

Fiber glass filaments are usually 2.0×10^{-4} to 1.0×10^{-3} inches in diameter. Fibers made from sodalime "A" glass are readily subject to moisture attack and therefore have limited storage life and strength. Requirements of fibers having high resistance to chemical attack and high strength are met by the commonly used Lime-Alumina-Borosilicate "E" glass.

Chart of Properties of "E" Glass

Physical Properties	
Specific gravity	2.55
Hardness	6.5 Moh Scale
Mechanical Properties	
Tensile strength	400,000 lb/in^2
Modulus of elasticity (tension)	10.5×10^6 lb/in^2
Bulk modulus	5.0×10^6 lb/in^2
Poisson's ratio	0.22
Hysteresis	None
Creep	None
Resilience modulus	7600 $in\text{-}lb/in^3$
Thermal Properties	
Coefficient of thermal expansion	$2.8 \times 10\text{-}6/F^o$
Coefficient of thermal conductivity	7.2 BTU $in/ft^2/hr/F^o$
Specific heat	0.19
Optical Properties	
Refractive index	1.548 (at 550 millimicrons at 32°C)

In manufacturing fibers from glass by a mechanical drawing process, small marbles of glass are formed which are free from all impurities. These marbles are heated in an electric furnace until they become molten. The molten glass flows through orifices in a small bushing at

the base of the furnace. During the early stage of cooling, the molten glass is made into filaments by mechanical drawing at a very high speed in the range of 5000 to 10,000 f.p.m. A surface trating material called "size" is applied to the filaments at the gathering device, which collects the filaments into a bundle known as "strands". The strands are twisted and wound into different styles of weaves (Figures 1 through 4).

RESINS

The most common resins which are available for use with glass filaments are polyesters, epoxies, phenolics, and silicones. Where high strength and abrasion-resistance are the main requirements, epoxy resins are predominant. Generally, the minimum amount of resin should be used to wet the filament. The sizing on the glass filament should be compatible with the resin to allow a good bond. The chemistry and general properties of all resins used for fiber glass reinforced plastics can be found in any standard book on resins.

FIBER GLASS REINFORCED LAMINATES

The physical properties and structural behavior of the laminates are primarily dependent upon sizing, the type and orientation of reinforcement, the volume of glass content present and the resin and molding methods for fabrication. The reinforcing materials offer various kinds of arrangements: (1) unidirectional warp, (2) random fiber mat, and (3) a number of woven cloth patterns. From these materials a wide variety of selections can be made to suit the design requirements.

The high strength of fibrous glass (tensile strength of about 400,000 p.s.i.) places it in the domain of structural materials. It obeys Hooke's law up to rupture, so this characteristic indicates that the structural material will either spring back to its original position or will fracture. This inherent property of fiber glass reinforced plastics can be used to advantage in designs involving shock absorption where temporary deformation can be tolerated. This characteristic makes it a most desirable material for landing gear struts for aircraft.

Another significant characteristic is the simplicity in fabricating the most intricate structural parts. This eliminates the complex load-carrying joints and thus improves the performance and dependability of the complete structure.

The low modulus of elasticity of fiber glass reinforced plastics was one of the main factors which restricted its application to primary structures for aircraft, but the rigorous requirements of military and space vehicles have led to the discovery of a high modulus glass which contains a small amount of BeO in the glass composition. The high

modulus glass fiber YM-31A (reference 11) has a 25-50 percent higher modulus of elasticity than "E" glass.

VARIATION OF MECHANICAL PROPERTIES WITH LAMINATE THICKNESS

There is a substantial reduction in tensile, compressive and flexural strength for thin laminates, particularly those less than about 1/32-inch. The reason for reduction is not clear, but one concept suggests(reference 12) that a portion of thickness at the surface is weaker than the interior of the laminate. This weak surface layer may be assumed to be more or less constant in thickness, regardless of the total thickness of the laminate. It constitutes a larger portion of thin laminates, than of thick laminates, and thus the strength properties may be expected to decrease with decreasing laminate thickness.

Data giving the fundamental mechanical properties reduced to a wet condition of 1/8-inch-to-1/4-inch-thick laminates are given in ANC-17. Semi-empirical relations are developed to calculate the strength of thin laminates.

The relation between strength and thickness for compression may be expressed as

$$F = F_m - k/t , \tag{1}$$

where F_m = maximum stress of a thick laminate for a thickness of 1/4 inch. This becomes

$$F_{1/4} = F_m - 4k .$$

Therefore, the ratio of the strength at any thickness "t" to that at 1/4 inch is expressed as

$$\frac{F}{F_{1/4}} = K_{F_C} = \frac{1 - \frac{k}{F_m}\frac{1}{t}}{1 - \frac{4k}{F_m}} \tag{2}$$

Also, for modulus of elasticity

$$\frac{E}{E_{1/4}} = K_{E_C} = \frac{1 - \frac{k}{E_m}\frac{1}{t}}{1 - \frac{4k}{E_m}} \tag{3}$$

If the data for a given laminate at two thicknesses are available, the parameters F_m and k can be calculated from equation (1). In case data for more than two thicknesses are available, the values of these parameters can be evaluated by the least square method.

$$F_m = \frac{\Sigma F \Sigma \frac{1}{t^2} - \Sigma \frac{F}{t} \Sigma \frac{1}{t}}{n \Sigma \frac{1}{t^2} - \left(\Sigma \frac{1}{t}\right)^2}, \quad k = \frac{\Sigma F \Sigma \frac{1}{t} - n \Sigma \frac{F}{t}}{n \Sigma \frac{1}{t^2} - \left(\Sigma \frac{1}{t}\right)^2},$$

where F = strength at some thickness "t" and n = number of values of F.

In case of modulus of elasticity, the equations are modified by replacing the strength term "F" by the modulus of elasticity term "E".

DESIGN CONSIDERATIONS FOR LAMINATES

To obtain maximum structural efficiency and economic utilization of glass fabric laminates, particularly for aircraft structures, selection of the best possible basic materials and thorough knowledge of the behavior of the material at various angles to the direction of the loading are required. When the empirical strength data are made available, based upon theoretical analysis, the designer can apply this material properly for structural uses in aircraft.

In designing glass fabric laminate, a few important assumptions are made. The first and most fundamental is that the glass and resin are firmly bonded together as one unit, and for any loading condition they undergo equal deformation. The second is that the material is considered to be elastic and obeys Hooke's law up to the point of rupture. The third is that all the fibers in the laminate are assumed to be straight and unstressed, or the initial stresses in the individual fibers are equal. This assumption in practice, however, is not quite true, as is seen from the tensile tests carried out on the test specimens. Some of the fibers break earlier and their loads are transferred to the unbroken fibers with the consequence that the failure of the laminate is caused by the successive breaking of the fibers rather than by simultaneous breaking of all of them. With improved fabricating techniques to make the fibers work together, the designer will be able to utilize higher stresses.

Another consideration is that most of the fiber glass laminates are orthotropic because of their layered construction. When the designer is provided with values of a number of elastic constants in addition to the strength properties of glass resin and combination, he is in a position to analyze the structure with suitably modified formulas (reference 9) based on the design theory of orthotropic materials.

EXPERIMENTAL INVESTIGATIONS

SPECIMENS

Since the major objective of the investigation was to obtain empirical buckling formulas of fiber glass reinforced plastic column members, the primary tests were directed towards the determination of these quantities. Secondary tests were carried out to check the quality of the material.

Twenty-four column specimens representing ten different lengths were tested. Each specimen was identified by "TP", followed by a hyphen and a number.

The specimens were fabricated in the Wood and Fiberglass Shop of the Aerophysics Department of Mississippi State University. Six plies of 181-glass Volan "A" cloth and American Cynamid 4154 Laminac polyester resin with 0.4 percent MEKP Catalyst were used to fabricate the required test members. The technique involved in fabricating the column members was a simple one. All the members were fabricated by hand lay-up process at room temperature.

The nominal mid-line dimensions of the cross sections were used for computation purposes. The check of the cross-sectional dimensions for each column member showed that although the sections were not absolutely uniform, the variation was small and the nominal dimensions formed the most satisfactory basis for computation of geometrical section properties.

The quality of the material was determined from the test coupons taken at random from apparently uninjured portions of test specimens. The properties of the material as determined from the tension and compression tests are summarized in Appendix I.

COLUMN TEST APPARATUS

The column tests were carried out in the 100,000-pound Riehle testing machine in the Civil Engineering Laboratory of Mississippi State University. The general arrangement for column tests is shown in Figure 5, which is a photograph of a 20-inch-long column under axial load. The load was applied to the specimen from the moving head of the testing machine through the upper end fitting.

The end fittings used to obtain the desired boundary conditions were specially designed and constructed in the Machine Shop of the Aerophysics Department at Mississippi State University. The main requirement was that the resultant load should be applied through the

centroid of the end cross section. Figure 6 shows the two end fitting assemblies. The pin-ended conditions were obtained by using two spherical steel balls of 1-inch diameter, each resting in between the two hardened steel plates at both the ends of the fittings, as shown in Figure 7. In order to prevent slipping of the steel balls during loading operation, small conical recesses were provided on the lower base plate of the lower block and on the upper base plate of the upper block. These base plates on which the two steel balls make contact were of hardened tool steel and were inserted into the aluminum blocks. This was done in order to reduce the weight of the end fittings.

Aluminum plugs - 1/2 inch in lenth, tapered down to 1/8 inch for fit and having a diameter equal to the inner diameter of the column members - were inserted exactly at the center of each block, which locates the central position of the struts in conjunction with the central line of the loading head of the machine. A special arrangement of two sets of clamps was used to provide for adjustment, whereby the steel balls could be adjusted along the line parallel to the centroidal axis of the end cross section of the strut so that the effect of initial eccentricities could be removed and a very sharply defined buckling of the strut could be obtained. This was done by lowering the upper end fitting (attached to the upper head of the machine) to have an exact alignment with the lower end fitting resting on the stationary platform of the machine. The two clamps on both the ends were not removed until an initial load of about 100 to 150 pounds was applied to the column test specimen. In this way it was ensured that the load acted along the center-line of both the end cross sections. Figure 8 shows the two clamps which locate the central position of the steel balls along the line parallel to the centroidal axis of the end cross section.

The bottom base block, 3/4-inch-thick, rested directly on the stationary platform of the machine while the heavy upper base block was fixed exactly at the central position of the movable head of the machine.

COLUMN TEST PROCEDURE AND RESULTS

After the individual test specimens were fabricated, the ends were squared and the edges of the cross sections broken with a fine file and fine sandpaper so that they rested smoothly on the flat surface of the end fittings. This was very necessary because, in the preliminary tests on short column members, it was observed that even a slight discrepancy in the evenness of the end cross section had lowered the failure load substantially.

After the specimen had been placed properly in the testing machine and sufficient load of about 100 to 150 pounds had been applied to take up all play, the end fittings were checked to make sure that the parts

were in their proper positions. Usually, some adjustment of the end position was found necessary, but this adjustment could be easily made as long as the axial load did not exceed 100 to 150 pounds. At this stage, the two clamps used to locate the central position of the steel balls were removed.

Once the specimen was properly located in the testing machine, the dial gauge, mounted on a stand, was adjusted at the center of the strut to find the central deflection of the column at each stage of loading. The initial reading of the dial gauge was recorded. The load was increased slowly to approximately half of the expected critical load. The load was then reduced to a convenient "basic load" for starting the test. At the same time the end fittings were again checked to make sure that the various parts were in proper relative position.

After the basic readings were completed the load was again increased at a slow rate. At convenient intervals, a set of readings were taken at the dial gauge to measure the central deflection of the column member.

Normal practice was to test two specimens having the same length. For short column members of length less than 15 inches, the central deflection observed was extremely small, but as the length of the specimen was increased, large deflections were observed.

Data from the four column members - 10, 15, 20, and 25 inches - seemed unreliable. An inspection showed that the strut had imperfections such as air bubbles which were not eliminated during the fabrication process and which caused a considerably lower load. The tests on these members were repeated, and the original data were essentially duplicated. Four additional members were fabricated to replace the four defective members.

In the case of the longer columns, a load was reached after which a small increase in load produced a large increase in deflection. This load was accepted as representing the buckling load of the column member. The details about the specimen tested are given in Table I.

Experimental determination of the elastic buckling stress is generally made on Southwell's assumption of hyperbolic relation between load and deflection (reference 16). It is presumed that a small amount of initial imperfection is inherent in the test specimens and this deviation from straight form goes on increasing with the load. According to theoretical assumptions, the load deflection relationship is given by two straight lines: the ordinate "OA" and a horizontal line at "A" parallel to the abscissa (Figure 9a), where "A" corresponds to the critical load. In practical cases, however, the expectation of sudden buckling at the critical load is not likely to be fulfilled. The initial deflection due to inaccuracies of fabrication or loading is intensified by the action of the applied forces. Within the region of small deflec-

tions, the load deflection curve approximates a rectangular hyperbola having the axis of zero deflection as an asymptote. Plotting δ/P against δ, where δ is the deflection and P the applied load, a straight line relationship is obtained - the inverse slope of which gives Pcr (shown in Figure 9b). The test results of column member TP12 plotted in Figures 10a and 10b show close agreement with the results predicted by theory. Similar results were obtained for other members, as given in Table II and shown graphically in Figure 11.

TYPES OF FAILURE

The failure encountered by the longer column members in compression was evidently Euler buckling. It was observed that after the column had reached its maximum load, a small increase in load produced a large increase in deflection. The action of a 40-inch-long column at different stages of loading, which indicates the Euler buckling, is shown in Figures 12 through 14.

Specimens less than 15 inches long did not show much deflection to the naked eye; however, small deflections were recorded from the dial gauge. The failure of a 10-inch specimen is shown in Figure 15.

The complete data recorded for the buckling of the column members are given in Table II.

TENSION AND COMPRESSION TESTS OF THE MATERIAL

The quality of the material was determined by carrying out tension and compression tests on the test coupons which are summarized in Appendix I. The stress-strain curves for compression and tension tests are given in Figures 16 through 18. It is interesting to note that, unlike isotropic materials, the behavior of fiber glass reinforced plastics in tension is different from compression.

DISCUSSION OF RESULTS

Certain physical laws are common to all columns. Within the elastic limit of the material, the primary buckling stress for column members of uniform cross section is given by Euler's formula.

$$\frac{P}{A} = C \frac{\pi^2 E}{(l/e)^2},$$

where P = maximum load on the column, lbs

A = cross-sectional area of the column, in^2

L = length of the column, in

ℓ = radius of gyration, in

$\frac{L}{\ell}$ = slenderness ratio

C = factor depending upon the end conditions (for pin-ended conditions C = 1)

From the elastic limit to the point of maximum stress, the curve which represents the load a column will support depends upon the characteristics of the material as well as the slenderness ratio.

The curve which was obtained can be represented by

$$\frac{P}{A} = \sigma_{max} - e\left[2.214(L/e)^4 - 120.4(L/e)^3 - 6374.0(L/e)^2 + 552460.0(L/e)\right] \times 10^{-6}$$

$$0 < L/e < (L/e)_{cr}$$

$$\frac{P}{A} = 0.875 \frac{\pi^2 E_a}{(L/e)^2}$$

$$(L/e) > (L/e)_{cr}$$

where $(L/e)_{cr} = 4.275\sqrt{\frac{E_a}{\sigma_{max}}}$

and $E_a = 0.92E$

The curve shown in Figure 11 is similar to the Forest Products Laboratory parabolic curve for plywood columns (reference 10); however, in Figure 11 the curve in the intermediate column range is steeper than the one obtained by the formula given in reference 10. It is quite likely that this might be due to either initial inherent imperfections of the column members, errors in testing procedures, i.e., eccentric loading, minor errors in boundary conditions or a combination of these factors. The amount of scattering of the plotted points, especially in the intermediate column range, justifies these reasons.

The degree of accuracy with Euler columns is believed to be primarily a matter of refinement used in determining the stiffness of the test specimens.

THEORETICAL CONSIDERATIONS FOR EFFICIENCY COMPARISON

The structures of maximum structural efficiency, or structures of minimum weight, are gnerally designed on the basis of simultaneous failure occurring in all modes which are critical. Any instability of a thin-walled compression member subjected to an axial thrust is generally considered a failure. Hence, there can be, in general, three types of failures: (1) primary buckling which can occur at stresses below the elastic limit (Euler buckling) or at stresses above the elastic limit (reference 18), (2) secondary or local buckling, and (3) material failure. Thus, the optimum section is derived by equating the primary buckling stress and local buckling stress to the compression stress of the material.

It can be shown that for a given load and allowable stress, considering primary buckling only, indefinite reduction in weight is possible by decreasing the thickness and suitably increasing the other sectional dimensions. However, reduction in thickness below a certain limit results in local instability failure. Thus, there is an optimum thickness which will be small enough to make the weight a minimum and at the same time large enough to prevent local buckling.

Three types of sections - circular cross section (Figure 19a), rectangular cross section (Figure 19b), and square cross section (Figure 19c) - have been treated in the analysis.

The relevant formulas for critical stress corresponding to the above modes of failure are given as

$$\sigma_{cc} = C\frac{\pi^2 E r}{(L/e)^2} = C\frac{\pi^2 E r}{L^2}\frac{I}{A}$$

$$(\sigma_{ccr})_{flat} = K_1 \bar{E}\left(\frac{t}{b}\right)^2$$

$$(\sigma_{ccr})_{circular} = K_2 \bar{E}\left(\frac{t}{R}\right)$$

$$\sigma = \frac{P}{A},$$

where C is the column end fixity and is equal to 1.0 for pin-ended columns.

K_1 = a nondimensional coefficient in local buckling formula for flat plate.

K_2 = a nondimensional coefficient in local buckling formula for circular plate.

E_r = reduced modulus.

$\bar{E}$ = effective modulus.

A. Circular Section

$$\sigma_{cc} = C\frac{\pi^2 E_r}{L^2}\cdot\frac{R^2}{2} \tag{1a}$$

$$\sigma_{ccr} = \frac{K_2\bar{E}}{D/t} \tag{1b}$$

$$\sigma = \frac{P}{2\pi Rt} \,. \tag{1c}$$

Imposing the condition $\sigma = \sigma_{ccr} = \sigma_{cc}$,

$$\frac{P}{2\pi Rt} = C\frac{\pi^2 E_r}{L^2}\,\frac{R^2}{2} = \frac{K_2\bar{E}}{D/t} \,. \tag{1d}$$

Solving for D and t from equation (1d),

$$D = 2\left[\frac{K_2 P L^4 \bar{E}}{C^2\pi^2 E_r^2}\right]^{1/6}, \quad t = \left[\frac{P}{K_2\pi\bar{E}}\right]^{1/6} .$$

From these two relations the value of optimum D/t can be obtained by substituting $\bar{E} = \sqrt{EE_r}$:

$$(D/t)_{opt} = 2\left[\frac{K_2^2 E}{C^2\pi(P/L^2)}\right]^{1/3} . \tag{1e}$$

Equation (1e) shows that for all alloys having the same base material the optimum D/t ratio is a function of the structural index only. Assuming a value of 0.4 for K_2 and unity for C, equation (1e) has been plotted in Figure 20 for various materials.

The primary buckling given by equation (1a) contains a design variable L. The term ℓ^2 is governed by the shape of the cross section, but it cannot be used for shape parameter because it is dimensional. Then we replace ℓ^2 by a nondimensional factor that depends upon the proportion of the cross section.

Since ρ^2 has the dimensions of an area, it may be divided by the cross-sectional area of the column to obtain the shape parameter k_1:

$$k_1 = \frac{\rho^2}{A} = \frac{D}{8\pi t}. \tag{1f}$$

Equation (1a) may thus be written as

$$\sigma_{cc} = \frac{\pi^2 E_r}{L^2} A k_1 . \tag{1g}$$

Substituting the values of k_1 and A where A is expressed in terms of load and stress $\sigma = P/A$; equation (1g) becomes

$$\sigma_{cc} = \frac{\pi^2 E_r}{L^2} \frac{P}{\sigma} \frac{D}{8\pi t} . \tag{1h}$$

The maximum stress that can be developed in circular column members can be obtained by substituting the value for (D/t) in equation (1h):

$$\sigma_{cc}^2 = \frac{\pi^{2/3}}{4} K_2^{2/3} E_r E^{1/3} (P/L^2)^{2/3} . \tag{1i}$$

Substitute $\tau = E_r/E$, since for a given material, τ is a known function of σ, which is plotted in Figures 21 through 25 for different materials.

Thus equation (1i) reduces to

$$\sigma_{cc} = \frac{\pi^{1/3}}{2} K_2^{1/3} \tau^{1/2} E^{2/3} (P/L^2)^{1/3} \tag{1j}$$

$$W_{opt} = (\text{area})_{opt} \times (\text{density})$$

$$= \frac{2}{\pi^{1/3}} \frac{P^{2/3} L^{2/3}}{K_2^{1/3} E^{2/3} \tau^{1/2}} \times \omega , \tag{1k}$$

where w = density of the material.

Efficiency η Criterion

From equation (1j) and (1k), $W/P = 1.0/\sigma_{cc}/\omega$, σ_{cc}/ω thus provides a convenient efficiency criterion for computing the potentialities of different materials.

From equation (1k),

$$\eta = \frac{\sigma_{cc}}{\omega} \quad \frac{\pi^{1/3}}{2} \; K_2^{1/3} \; \frac{E^{2/3} \tau^{1/2}}{\omega} \left(\frac{P}{L^2}\right)^{1/3}, \tag{1l}$$

where $E^{2/3} \tau^{1/2}$ = material parameter and

$(P/L^2)^{1/3}$ = loading parameter.

Equation (1l) is plotted (Figure 26) as curves of η against $\sqrt{P/L^2}$ for different materials.

B. Rectangular Cross Section

$$\sigma_{cc} = C \frac{\pi^2 E_r}{L^2} \quad \frac{b^2 m^2 (3+m)}{3(1+m)} \tag{2a}$$

$$\sigma_{ccr} = K_1 \bar{E} \left(\frac{t}{2b}\right)^2 \tag{2b}$$

$$\sigma = \frac{P}{4bt(1+m)} \tag{2c}$$

where $m = h/b$.

Imposing the condition $\sigma_c = \sigma_{ccr} = \sigma_{cc}$,

$$\frac{P}{4bt(1+m)} = K_1 \bar{E} \left(\frac{t}{2b}\right)^2 = C \; \frac{\pi^2 E_r}{L^2} \; \frac{b^2 m^2 (3+m)}{3(1+m)}, \tag{2d}$$

and solving for b and t from equation (2d),

$$b = \left[\frac{27(1+m)}{64\pi^6 m^6 (3+m)^3}\right]^{1/10} \times \left[\frac{K_1 P^2 L^6 \bar{E}}{C^3 E_r^3}\right]^{1/10}$$

$$t = \left[\frac{3}{4\pi^2 m^2 (1+m)^3 (3+m)}\right]^{1/10} \times \left[\frac{P^4 L^2}{C K_1^3 \bar{E}^3 E_r}\right]^{1/10}.$$

From the above two relations, the value of optimum (b/t) can be obtained by substituting $\bar{E} = \sqrt{E E_r}$:

$$\left(\frac{b}{t}\right)_{opt} = \left[\frac{9(1+m)^4}{16\pi^4 m^4 (3+m)^2}\right]^{1/10} \frac{K_1^{2/5} E^{1/5}}{(P/L^2)^{1/5} C^{1/5}} \tag{2e}$$

Equation (2e) also shows that for all alloys having the same base material the optimum (b/t) ratio is a function of the structural index only. Assuming a value of 3.6 for K_1 and unity for C, equation (2e) has been plotted in Figures 27a through 27d for various ratios of h/b.

The shape parameter in this case is given by

$$k_1 = \frac{\ell^2}{A} = \frac{m^2(3+m)}{12(1+m)^2}\left(\frac{b}{t}\right). \tag{2f}$$

The primary buckling equation (2a) may thus be written as

$$\sigma_{cc} = \frac{\pi^2 E_r}{L^2} A k_1 \tag{2g}$$

substituting the values of k_1 and A, where A is expressed in terms of load and stress $\sigma = P/A$. Thus equation (2g) becomes

$$\sigma_{cc} = \frac{\pi^2 E_r}{L^2} \frac{P}{\sigma} \frac{m^2(3+m)}{(1+m)^3} \left(\frac{b}{t}\right)_{opt}. \tag{2h}$$

The maximum stress that can be developed in a rectangular cross section can be obtained by substituting the values for optimum (b/t) ratio in (2h):

$$\sigma^2 = 0.4912\, E_r K_1^{2/5} E^{1/5} (P/L^2)^{4/5} \frac{m^{8/5}(3+m)^{4/5}}{(1+m)^{8/5}}. \tag{2i}$$

$\tau = E_r/E$ is substituted, since for a given material, τ is a known function of σ, which has been plotted in Figures 21 through 25 for different materials. The equation (2i) reduces to

$$\sigma = 0.7008\, K_1^{1/5} \tau^{1/5} E^{3/5} (P/L^2)^{3/5} \frac{m^{4/5}(3+m)^{2/5}}{(1+m)^{4/5}} \tag{2j}$$

$$(W)_{opt} = (Area)_{opt} \times \omega$$

$$= 1.4270 \frac{(1+m)^{4/5}}{m^{4/5}(3+m)^{3/5}} \frac{P^{3/5} L^{4/5}}{K^{1/5} E^{2/5} \tau^{1/2}} \times \omega . \qquad (2k)$$

Efficiency η Criterion

From equations (2j) and (2k), $\frac{W}{P} = \frac{1.0}{\sigma_{cc}/\omega}$.

Thus σ_{cc}/w provides a convenient efficiency criterion for comparing the potentialities of different materials.

From equation (2k),

$$\eta = \frac{\sigma_{cc}}{\omega} = 0.7008 \frac{m^{4/5}(3+m)^{3/5}}{(1+m)^{4/5}} K_1^{1/5} \frac{E^{3/5} \tau^{1/2}}{\omega} (P/L^2)^{2/5}, \qquad (2\ell)$$

where $\frac{E^{3/5} \tau^{1/2}}{\omega}$ = material parameter and

$(P/L^2)^{2/5}$ = loading parameter.

Equation (2ℓ) is plotted in Figure 28 for h/b = m = 0.8 as curves of η against $\sqrt{P/L^2}$ For any desired ratio of h/b, such curves can be plotted.

C. Square Section

A square section is a special case of a rectangular cross section when m = 1. By substituting the value m = 1 in the analysis made for the rectangular cross section, we get

$$\left(\frac{b}{t}\right)_{opt} = 0.5973 \frac{K_1^{2/5} E^{1/5}}{(P/L^2)^{1/5} C^{1/5}}, \qquad (3a)$$

which is plotted in Figure 29.

Also, $$\eta = \frac{\sigma_{cc}}{\omega} = 0.7008 K_1^{1/5} \frac{E^{3/5} \tau^{1/2}}{\omega} (P/L^2)^{2/5}, \qquad (3b)$$

which is plotted in Figure 30.

COMMENTS

After having obtained the empirical column buckling formulas for fiber glass reinforced plastic materials, the column efficiency is compared with conventional structural alloys.

Efficiency equations (1ℓ), (2ℓ), and (3b) for circular, rectangular, and square cross-sectional members of different materials have been plotted against the loading parameter $\sqrt{P/L^2}$ in Figures 26, 28, and 30, respectively. To contract the scale, the square root of the structural index has been used for plotting.

A comparative study of Figure 30 for column members of square cross section shows that for lightly loaded structures, $P/L^2 < 14.0$ p.s.i., 143-glass fabric is the optimum material, while for heavily loaded structures, P/L^2 714.0 p.s.i., the lightest column would be from 7075 aluminum alloy. When 143-glass fabric is compared with 2024 aluminum alloy and fully hardened steel, it is shown to be much superior to these alloys in all the loading ranges. At $P/L^2 =$ 400 p.s.i., 143-glass fabric is 47 percent superior to 2024 aluminum alloy and 32 percent superior to fully hardened steel.

181 Volan "A" cloth is shown to be 36 percent inferior to 7075 aluminum alloy for $P/L^2 < 50.0$ p.s.i. loading range and 12 percent inferior to 2024 aluminum alloy at the low loading range of $P/L^2 < 9.0$ p.s.i. But 181-glass fabric is superior to fully hardened steel for lightly loaded structures for the loading range $P/L^2 < 25.0$ p.s.i.

Figure 30 is thus primarily of value only as indicating the general range of loading for which a material may have efficient applications.

A similar comparative study of column efficiency for circular and rectangular cross sections can also be made from Figure 26 and Figure 28.

CONCLUSION

The analysis made in this report is primarily directed towards studying the efficiency of column members of Volan "A" 181- and 143-glass fabrics, with 4154 polyester resin, in comparison with other metallic structural alloys.

Even though Young's modulus of 143-glass reinforced plastic (4.91×10^6 p.s.i.) is considerably low, the material shows great potential for column members. Particularly for the low loading range ($P/L^2 < 14.0$ p.s.i.), square column members of this material show optimum structural range; in other words, the efficiency is greater than any other comparable material.

Column members of Volan "A" 181-glass reinforced plastic do not show appreciable improvement in efficiency. This is because Young's modulus (2.916×10^6 p.s.i.) is very low.

When the special high modulus glass fabrics currently under development are fully developed, and better resins and improved molding techniques are known, it is reasonable to believe that glass reinforced plastics will become a highly feasible and competitive material for use as column members in aircraft structures.

Manufacturing considerations, rather than loading considerations, may also be a deciding factor for determining the most suitable material for a particular application.

Structures from reinforced plastics can be easily fabricated to the required optimum size by molding processes, thereby eliminating the considerable machining which is involved in many of the metallic alloy structures.

TABLE I
DIMENSIONS AND PROPERTIES OF COLUMNS

Test Sample	t (in)	I.D. (in)	A $(in)^2$	$\rho = \sqrt{I/A}$ (in)	L (in)	L/ρ
TP-01	0.0770	1.3250	0.3206	0.4684	8.550	18.25
TP-02	0.0770	1.3250	0.3206	0.4684	8.550	18.25
TP-03	0.0720	1.3270	0.3001	0.4691	10.150	21.64
TP-04	0.0725	1.3460	0.3066	0.4758	10.000	21.15
TP-05	0.0750	1.3450	0.3169	0.4755	10.000	21.03
TP-06	0.0700	1.3460	0.2960	0.4758	12.000	25.35
TP-07	0.0750	1.3420	0.3162	0.4744	12.000	25.43
TP-08	0.0725	1.3460	0.3066	0.4744	14.875	31.36
TP-09	0.0700	1.3475	0.2963	0.4763	15.000	31.50
TP-10	0.0800	1.3255	0.3331	0.4686	15.000	32.00
TP-11	0.0700	1.3300	0.2925	0.4702	20.100	42.75
TP-12	0.0725	1.3535	0.3083	0.4785	20.000	41.80
TP-13	0.0730	1.3455	0.3086	0.4756	20.000	42.17
TP-14	0.0750	1.3430	0.3164	0.4748	25.000	52.70
TP-15	0.0750	1.3430	0.3164	0.4748	25.000	52.70
TP-16	0.0725	1.3535	0.3061	0.4785	24.625	51.45
TP-17	0.0700	1.3450	0.2958	0.4755	25.000	52.57
TP-18	0.0750	1.3430	0.3164	0.4748	30.000	63.19
TP-19	0.0750	1.3450	0.3165	0.4755	30.000	63.19
TP-20	0.0800	1.3450	0.3380	0.4755	35.000	73.93
TP-21	0.0800	1.3450	0.3380	0.4755	35.000	73.93
TP-22	0.0720	1.3430	0.3038	0.4748	40.000	84.47

TABLE I - (Contd.)

Test Sample	t (in)	I.D. (in)	A $(in)^2$	$\ell = \sqrt{I/A}$ (in)	L (in)	L/ℓ
TP-23	0.0750	1.3410	0.3164	0.4740	45.000	94.94
TP-24	0.0750	1.3410	0.3164	0.4740	45.000	94.94

TABLE II
TEST RESULTS ON COLUMNS

Test Sample	t (in)	I.D. (in)	A $(in)^2$	L/ℓ	σ_{ult} (lb)	σ_{max} (lb/in^2)
TP-01	0.0770	1.3250	0.3206	18.25	10,150	31,660
TP-02	0.0770	1.3250	0.3206	18.25	10,200	31,850
TP-03	0.0720	1.3270	0.3001	21.64	7,000	23,325*
TP-04	0.0725	1.3460	0.3066	21.15	9,190	29,975
TP-05	0.0750	1.3450	0.3169	21.03	9.550	30,145
TP-06	0.0700	1.3460	0.2960	25.35	7,750	36,182
TP-07	0.0750	1.3420	0.3162	25.43	8,000	25,300
TP-08	0.0725	1.3460	0.3066	31.36	5,850	19,080
TP-09	0.0700	1.3475	0.2963	31.50	6,000	20,250
TP-10	0.0800	1.3255	0.3331	32.00	6,200	18,615*
TP-11	0.0700	1.3300	0.2925	42.75	3,500	11,966*
TP-12	0.0725	1.3535	0.3083	41.80	4,230	13,720
TP-13	0.0730	1.3455	0.3086	42.17	4,050	13,125
TP-14	0.0750	1.3430	0.3164	52.70	2,250	7,110*
TP-15	0.0750	1.3430	0.3164	52.70	2,750	8,700
TP-16	0.0725	1.3535	0.3061	51.45	2,900	9,475
TP-17	0.0700	1.3450	0.2958	52.57	2,725	9,210
TP-18	0.0750	1.3430	0.3164	63.19	2,000	6,325
TP-19	0.0750	1.3450	0.3165	63.19	2,050	6,475
TP-20	0.0800	1.3450	0.3380	73.93	1,500	4,438
TP-21	0.0800	1.3450	0.3380	73.93	1,510	4,470
TP-22	0.0720	1.3430	0.3038	84.47	1,050	3,456

TABLE II - (Contd.)

Test Sample	t (in)	I.D. (in)	A (in)^2	L/ℓ	σ_{ult} (lb)	σ_{max} (lb/in^2)
TP-23	0.0750	1.3410	0.3164	94.94	910	2,875
TP-24	0.0750	1.3410	0.3164	94.94	900	2,844

* The column members were defective.

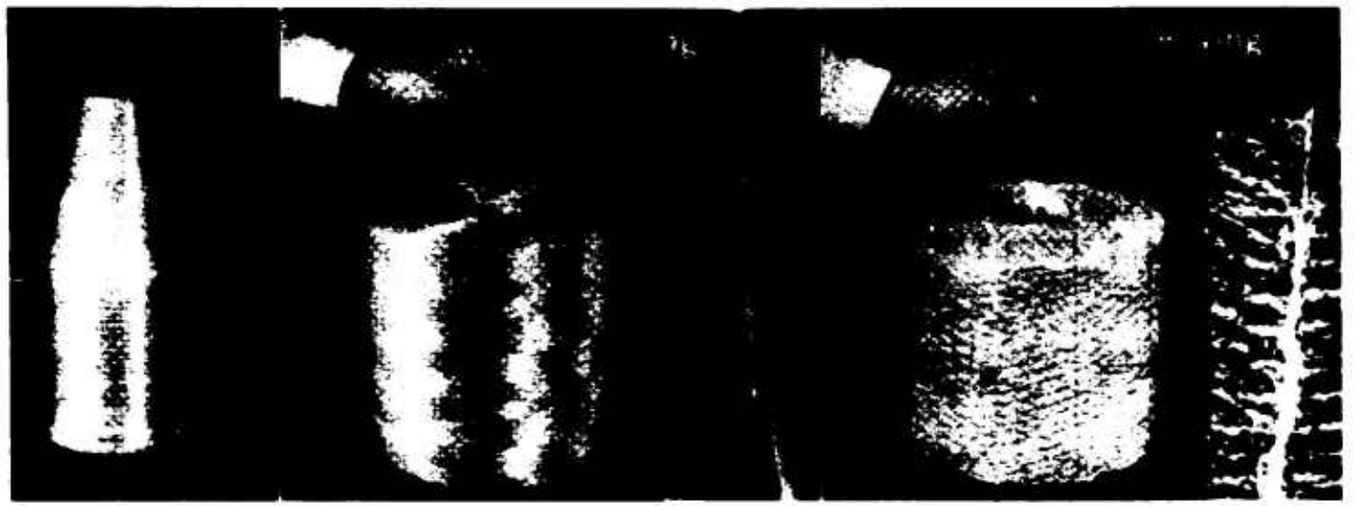

Figure 1. Continuous Strand.

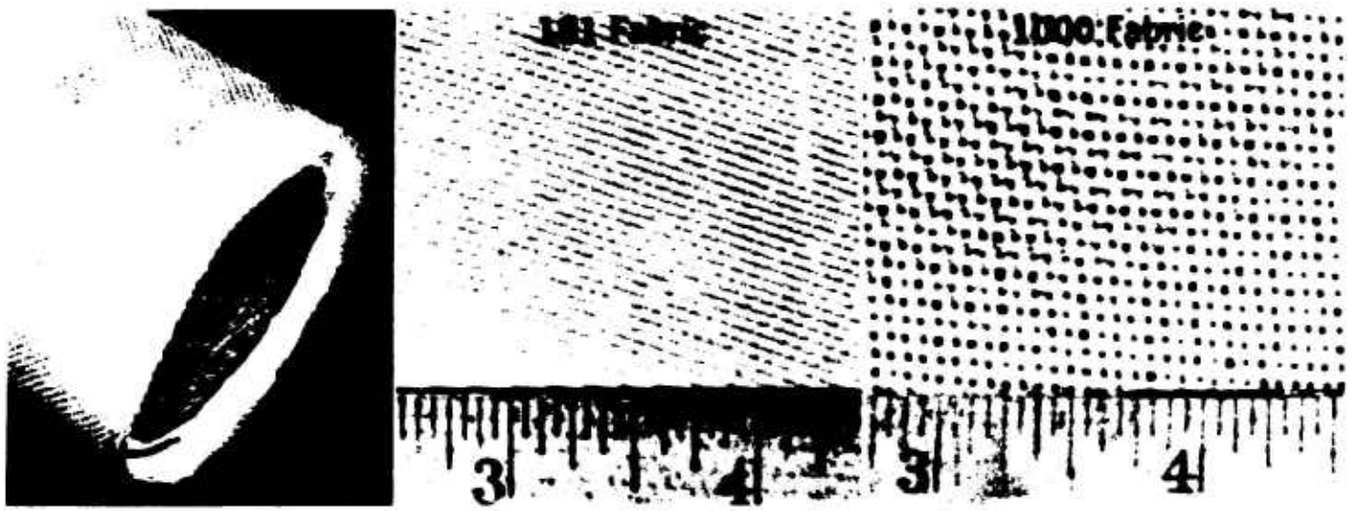

Figure 2. Fabrics.

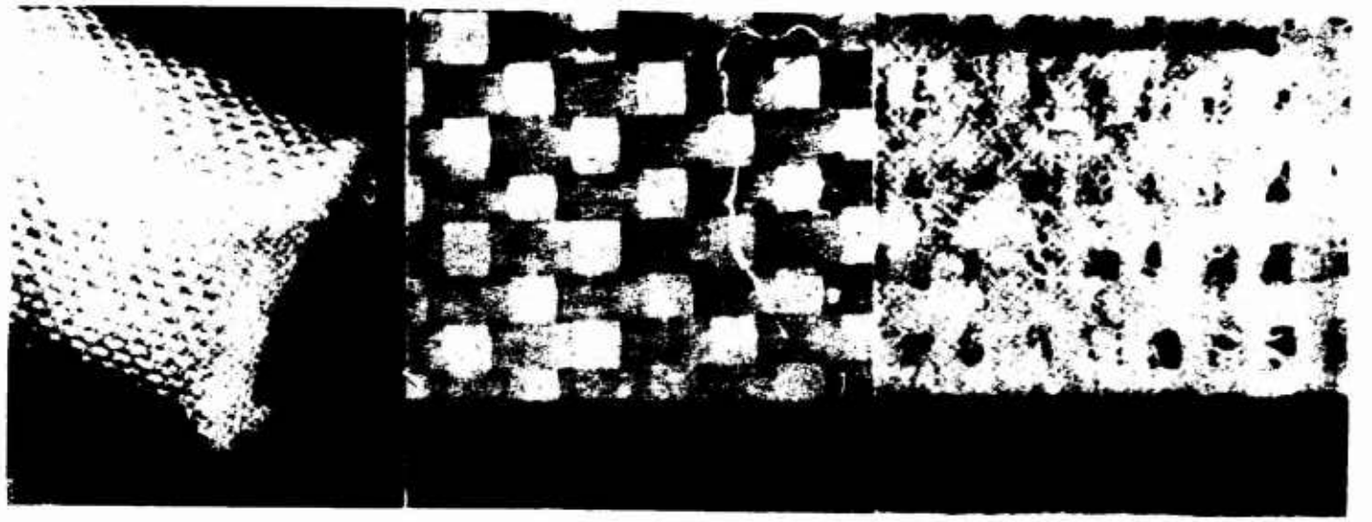

Figure 3. Woven Rovings.

Figure 4. Reinforcing Mats.

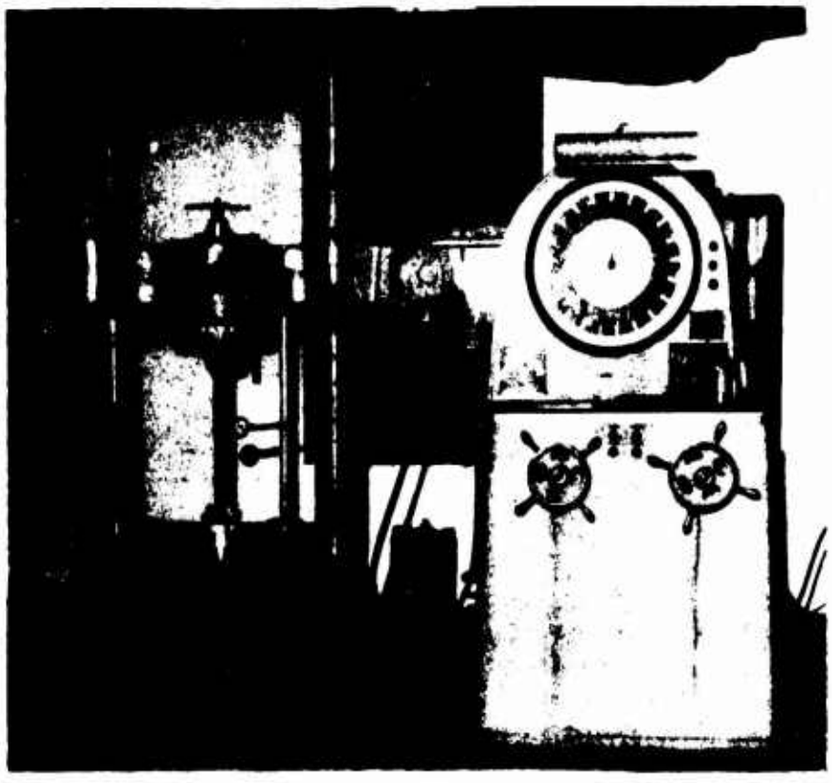

Figure 5. General Arrangement for Column Test.

Figure 6. End Fitting Assemblies.

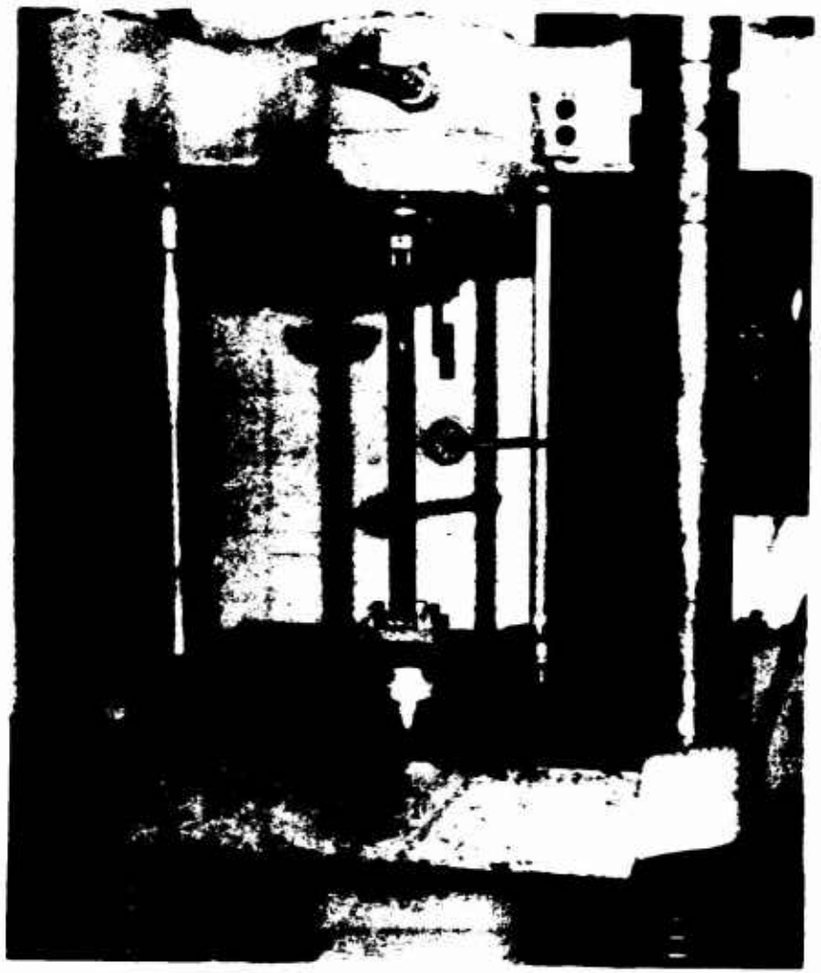

Figure 7. Pin-Ended Condition for Test Specimen.

Figure 8. Clamps Used to Locate the Central Position of the Steel Balls.

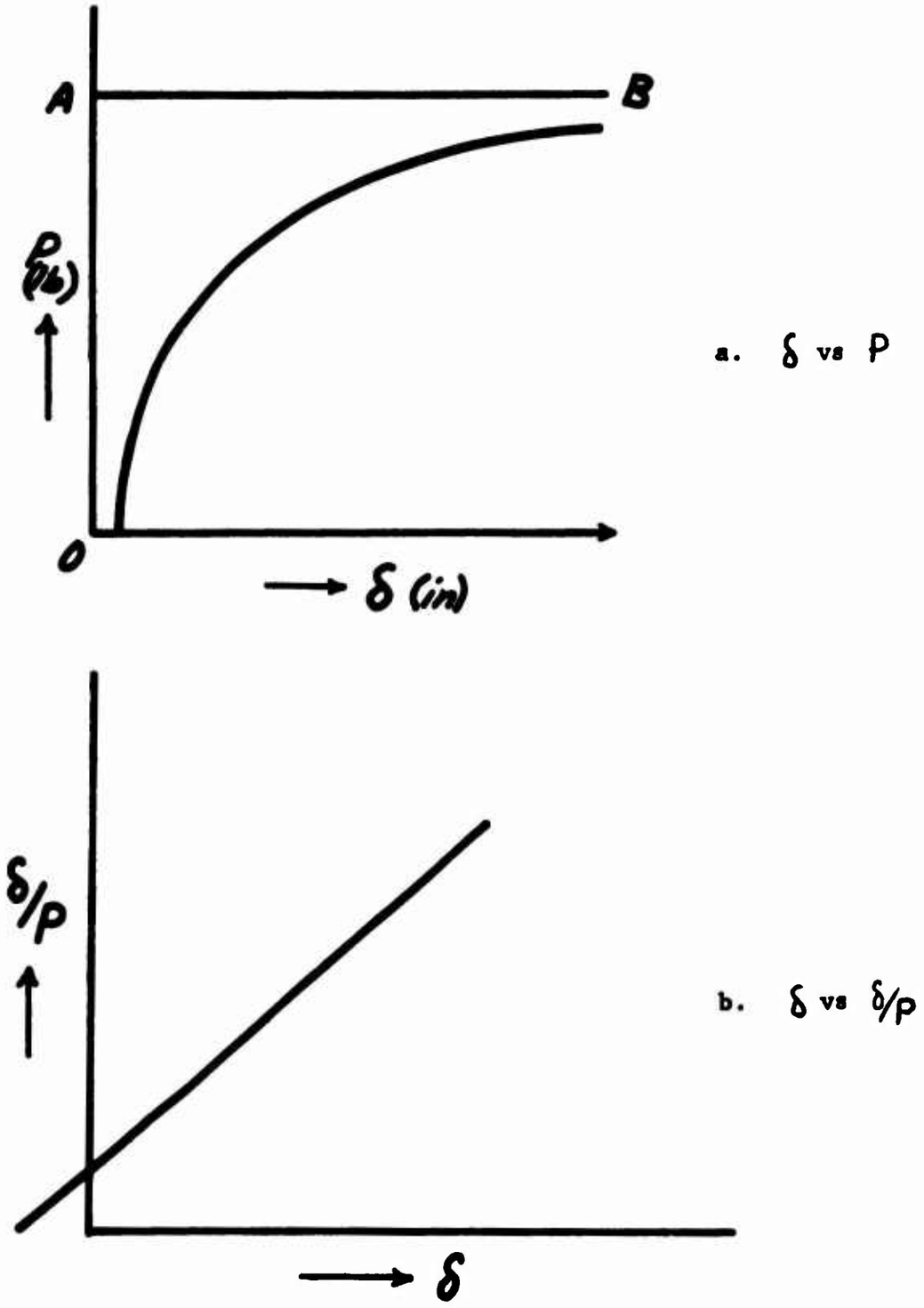

a. δ vs P

b. δ vs δ/P

Figure 9. Theoretical Curves of Deflection Versus Applied Load and Ratio of Deflection to Applied Load, Based on Southwell's Assumption.

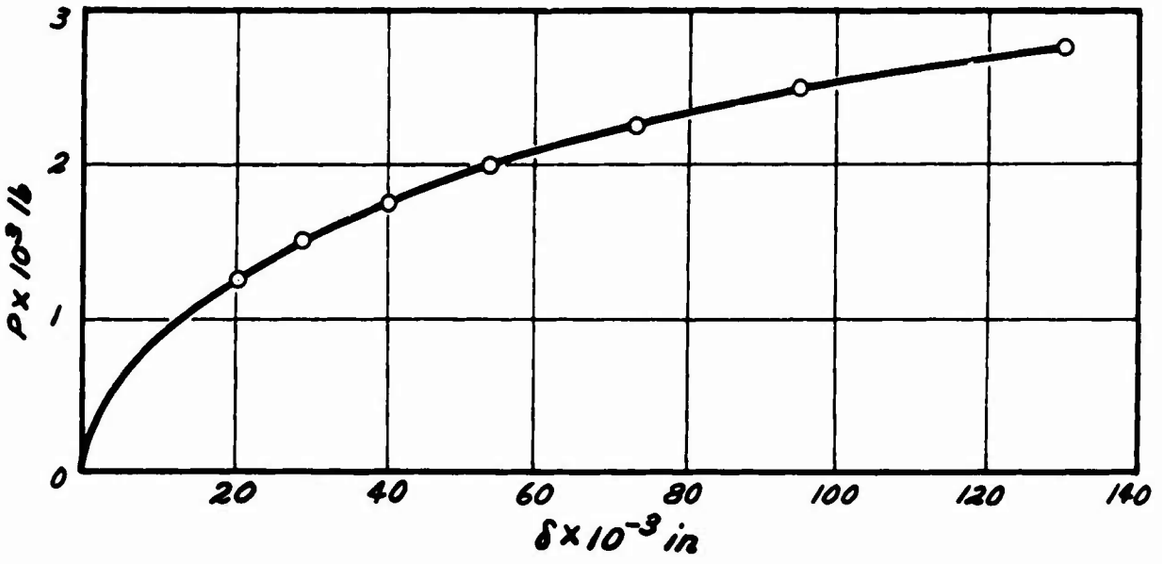

Figure 10a. Load Versus Deflection for 20.15-inch Specimen.

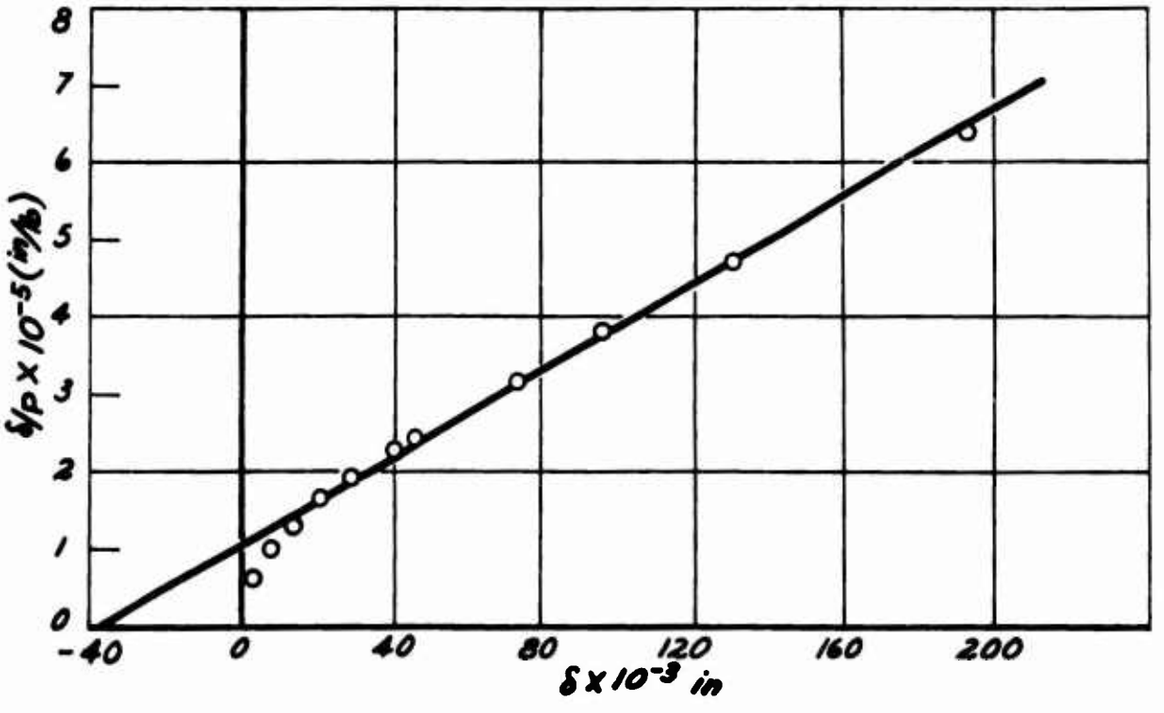

Figure 10b. Deflection Versus Ratio of Deflection to Applied Load for 20.15-inch Specimen.

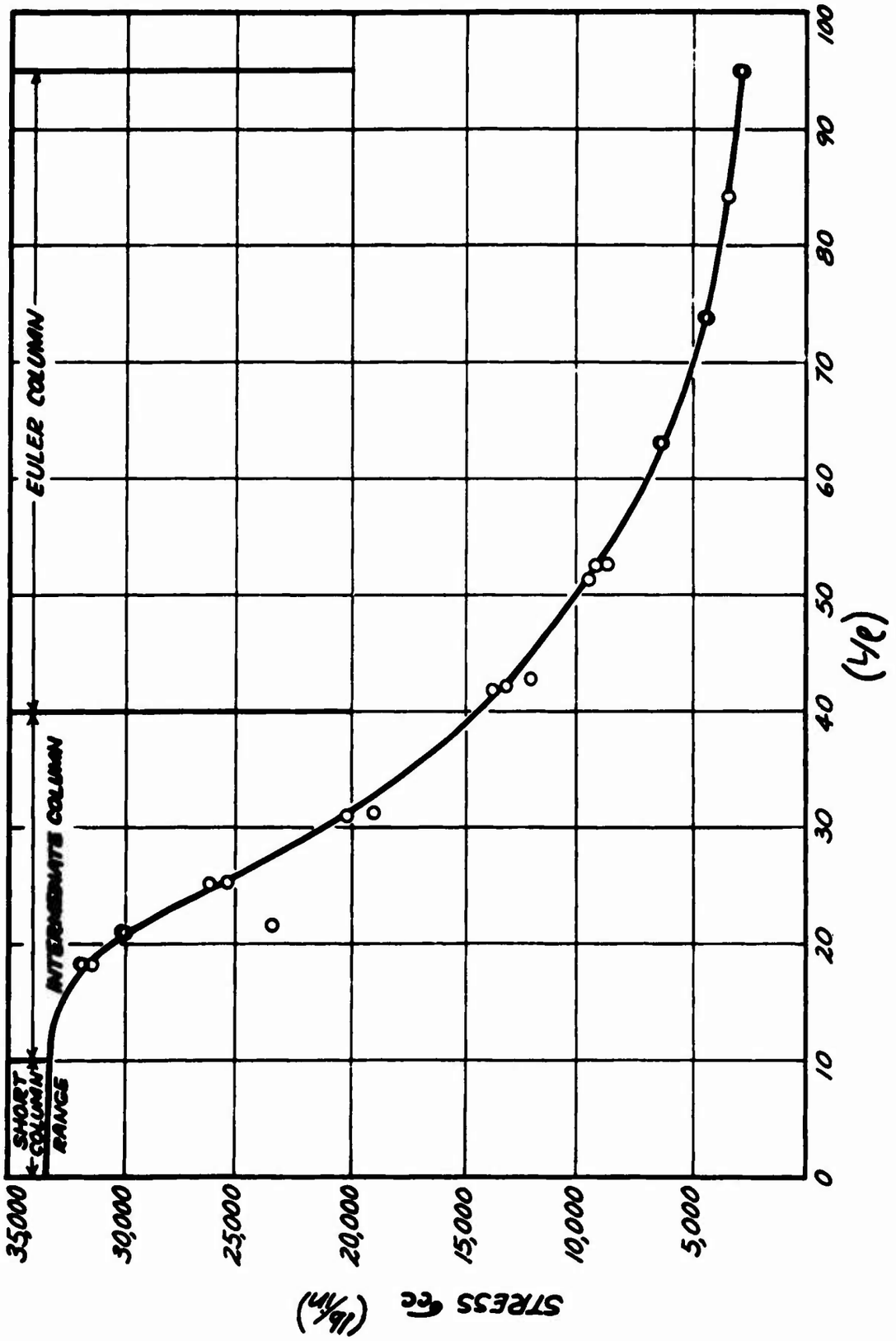

Figure 11. Experimental Column Buckling Curve for Fiber Glass.

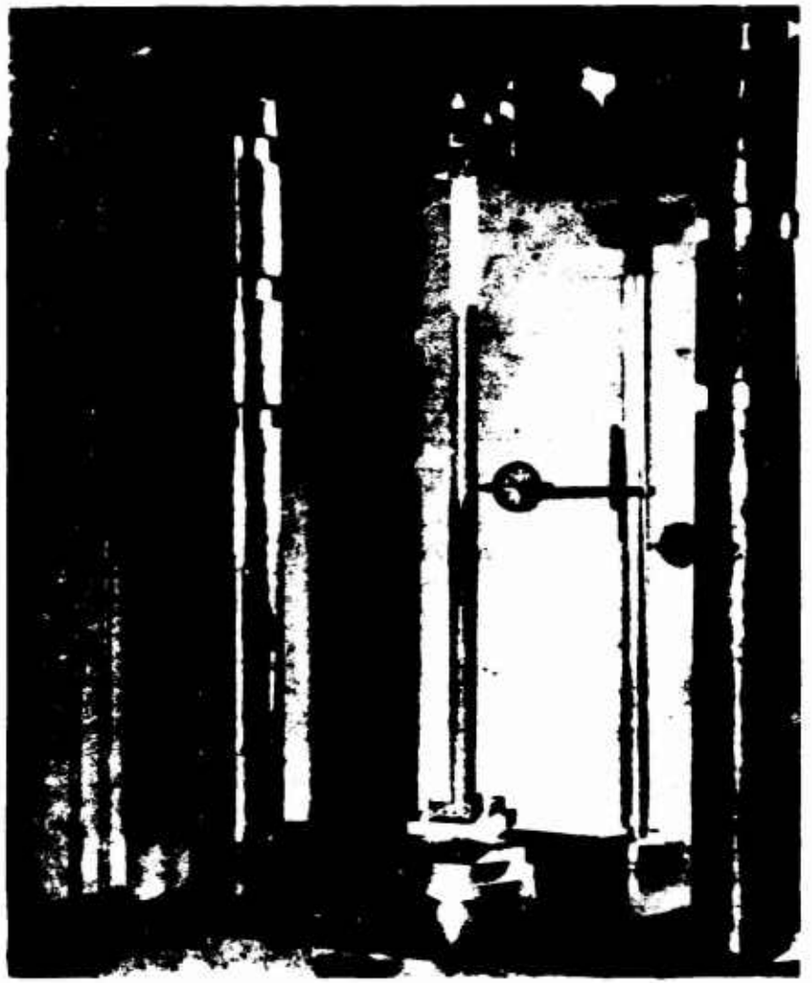

Figure 12. 40-inch Column Under Different Stages of Loading.

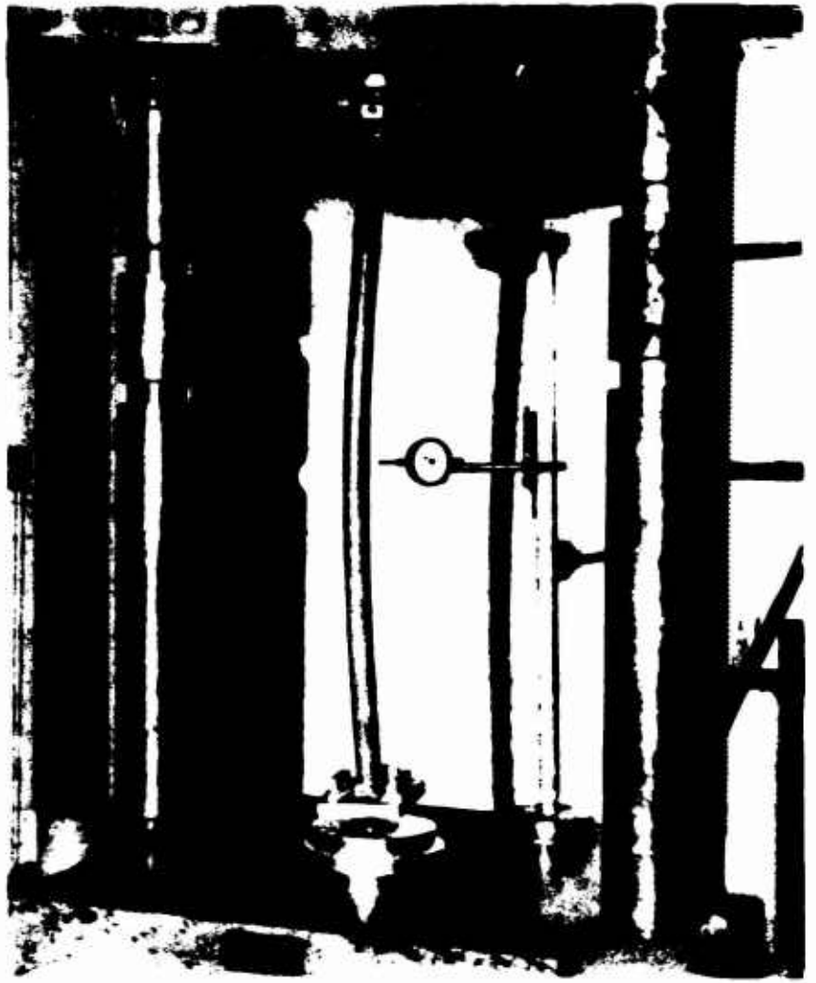

Figure 13. 40-inch Column Under Different Stages of Loading.

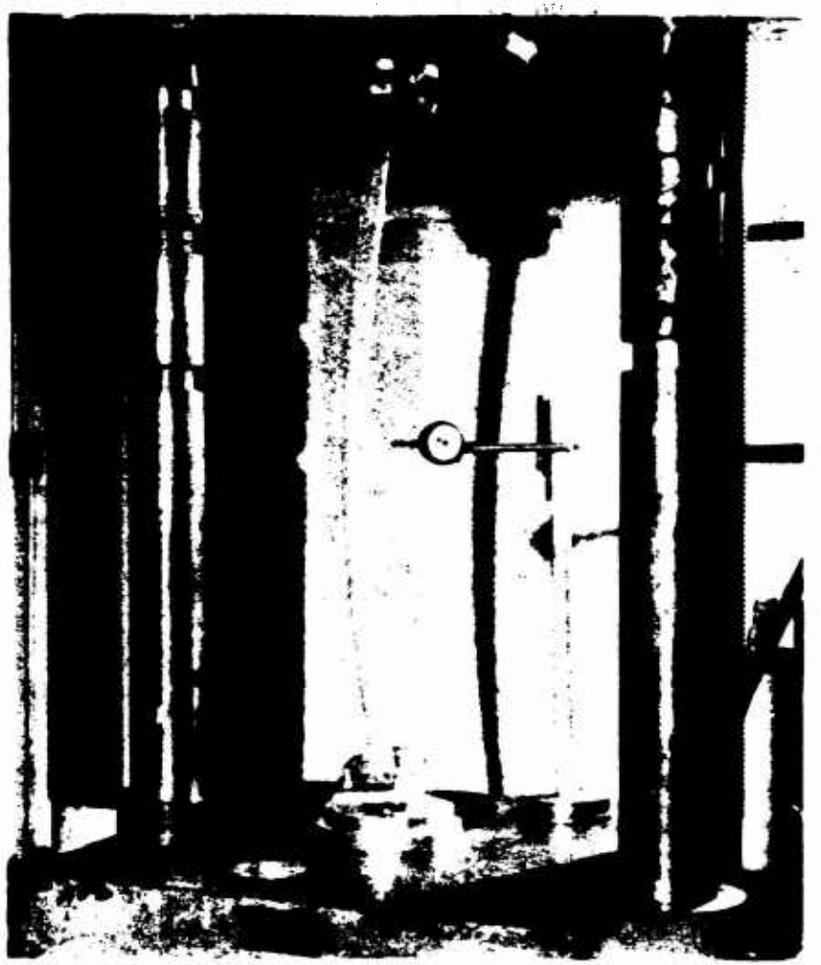

Figure 14. 40-inch Column Under Critical Load.

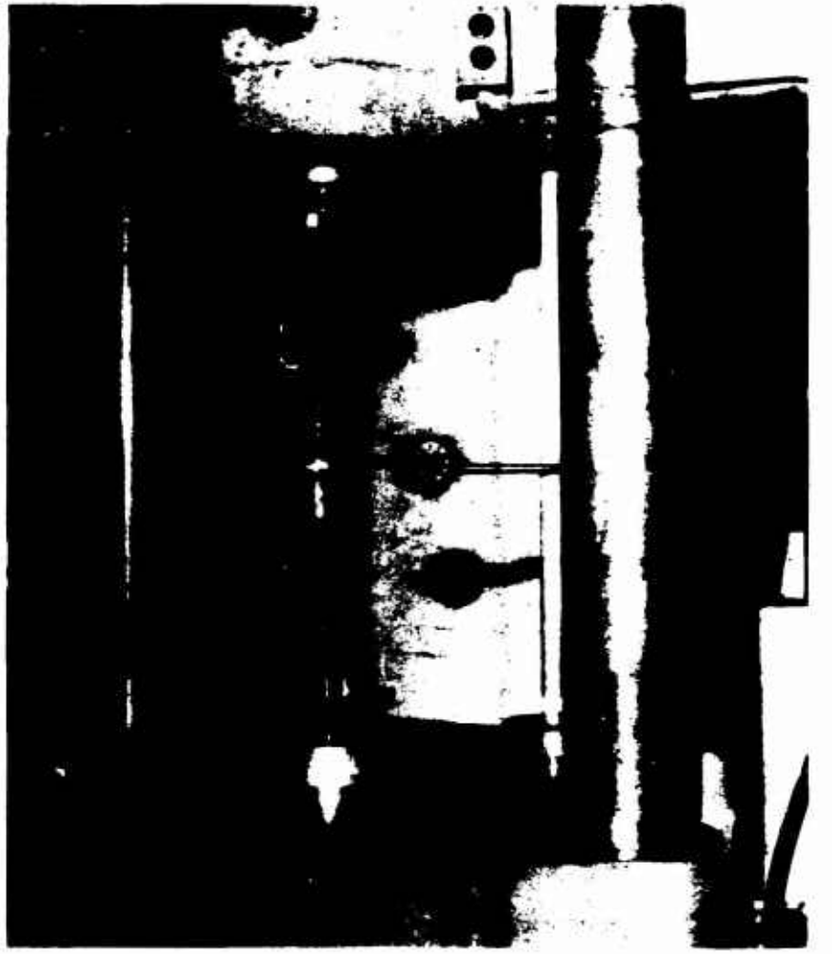

Figure 15. Failure of 10-inch Column.

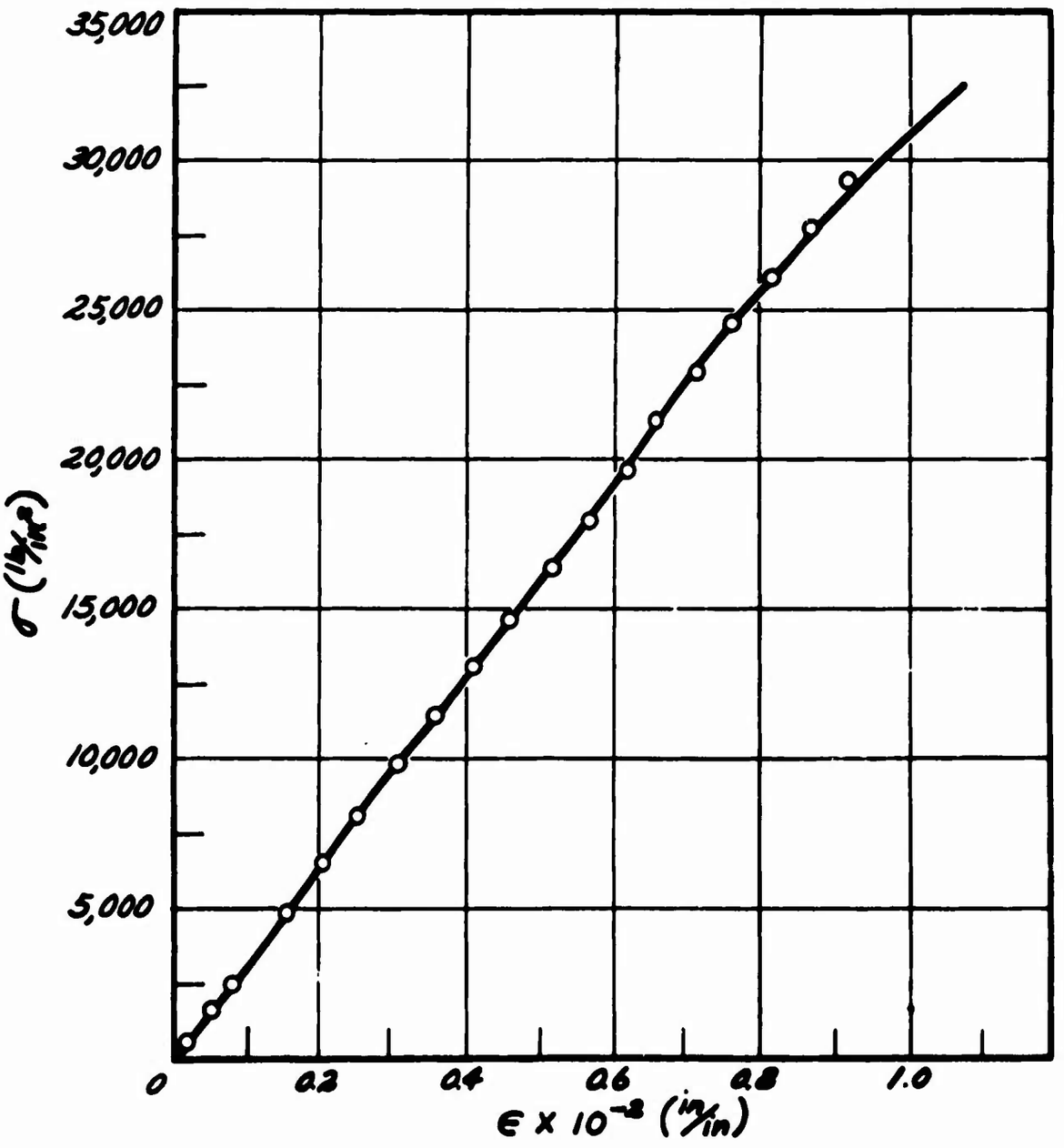

Figure 16. Stress-Strain Curve in Compression.

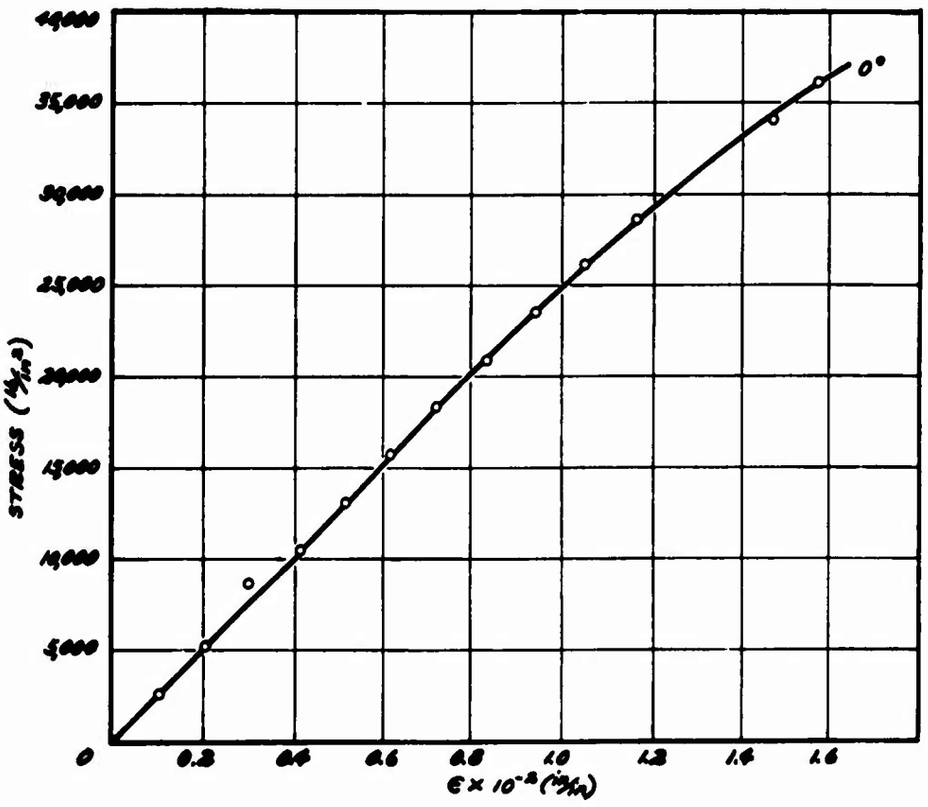

Figure 17. Stress-Strain Curve in Tension for an Angle Between Applied Load and Primary Direction of Fabric Equal to Zero Degrees.

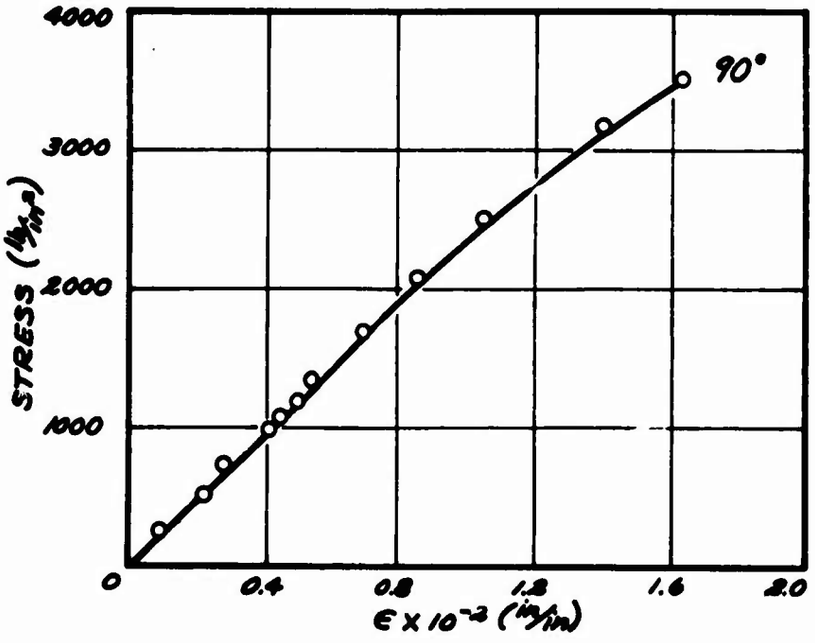

Figure 18. Stress-Strain Curve in Tension for an Angle Between Applied Load and Primary Direction of Fabric Equal to Ninety Degrees.

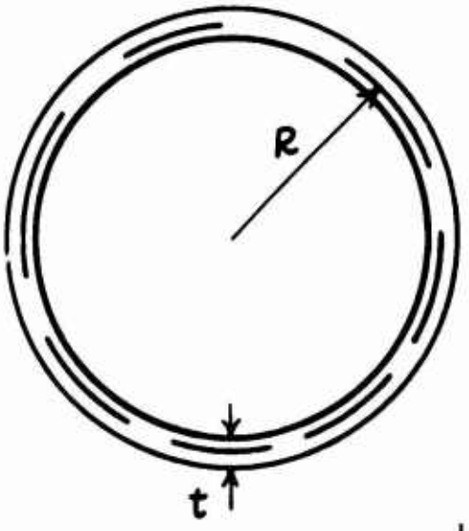

Figure 19a. Circular Section.

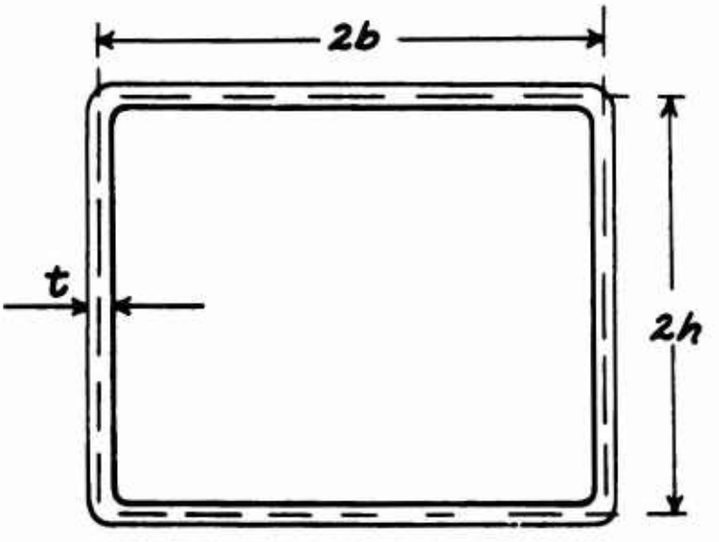

Figure 19b. Rectangular Section.

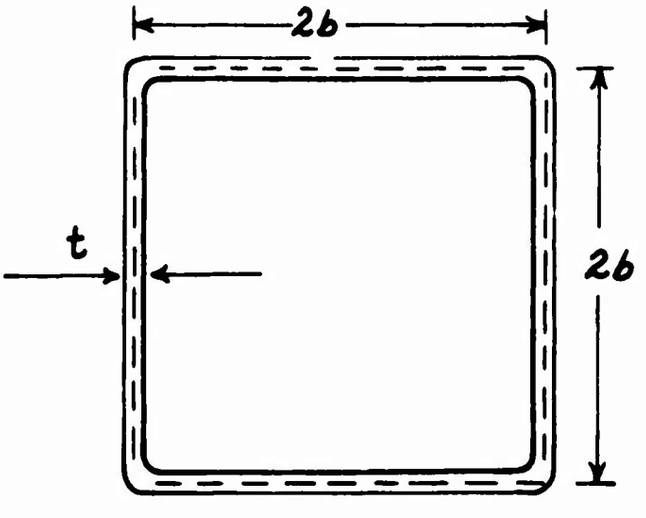

Figure 19c. Square Section.

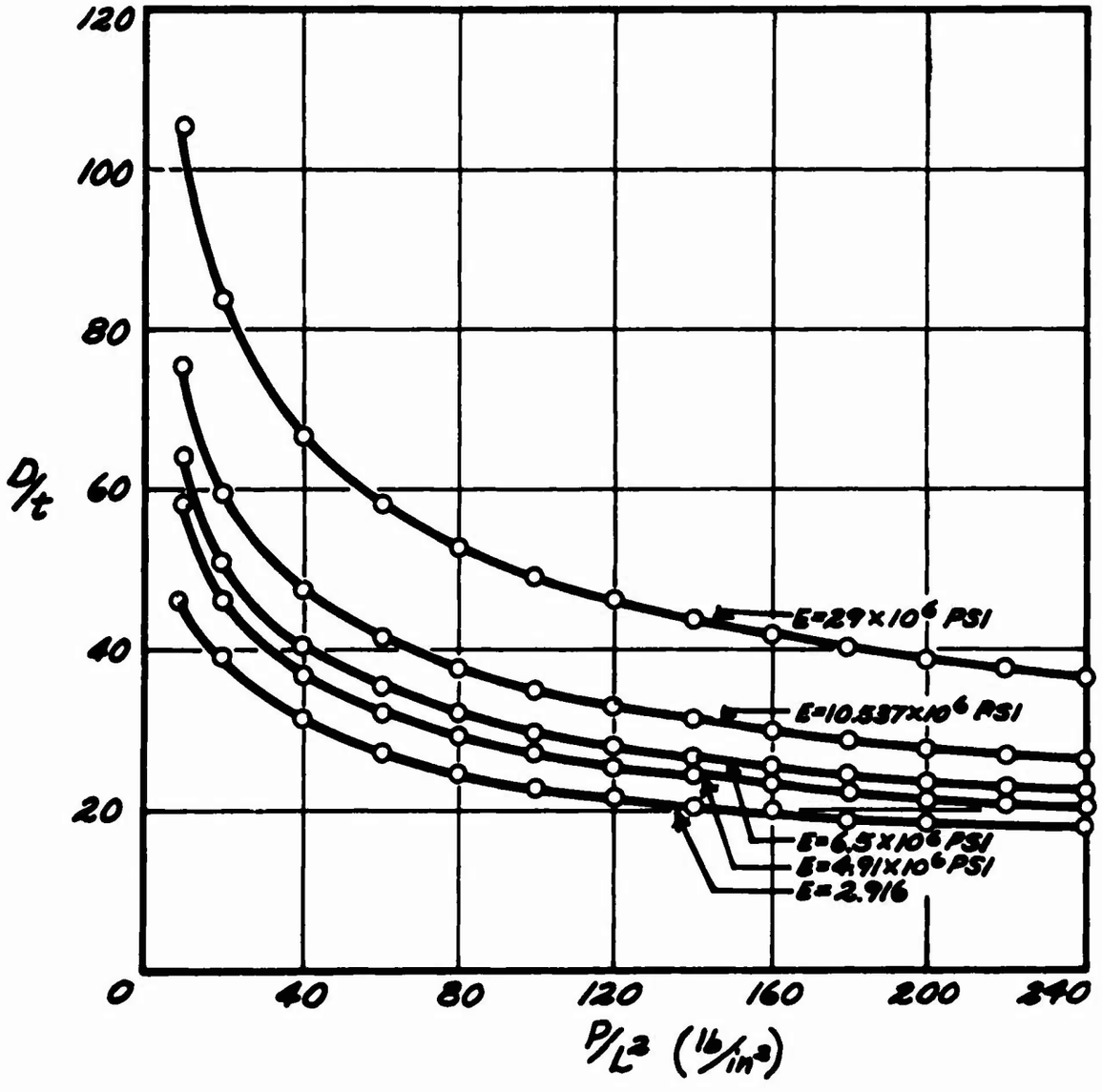

Figure 20. Ratio of Applied Load to Column Length Squared Versus Ratio of Tube Diameter to Thickness for Circular Column Members.

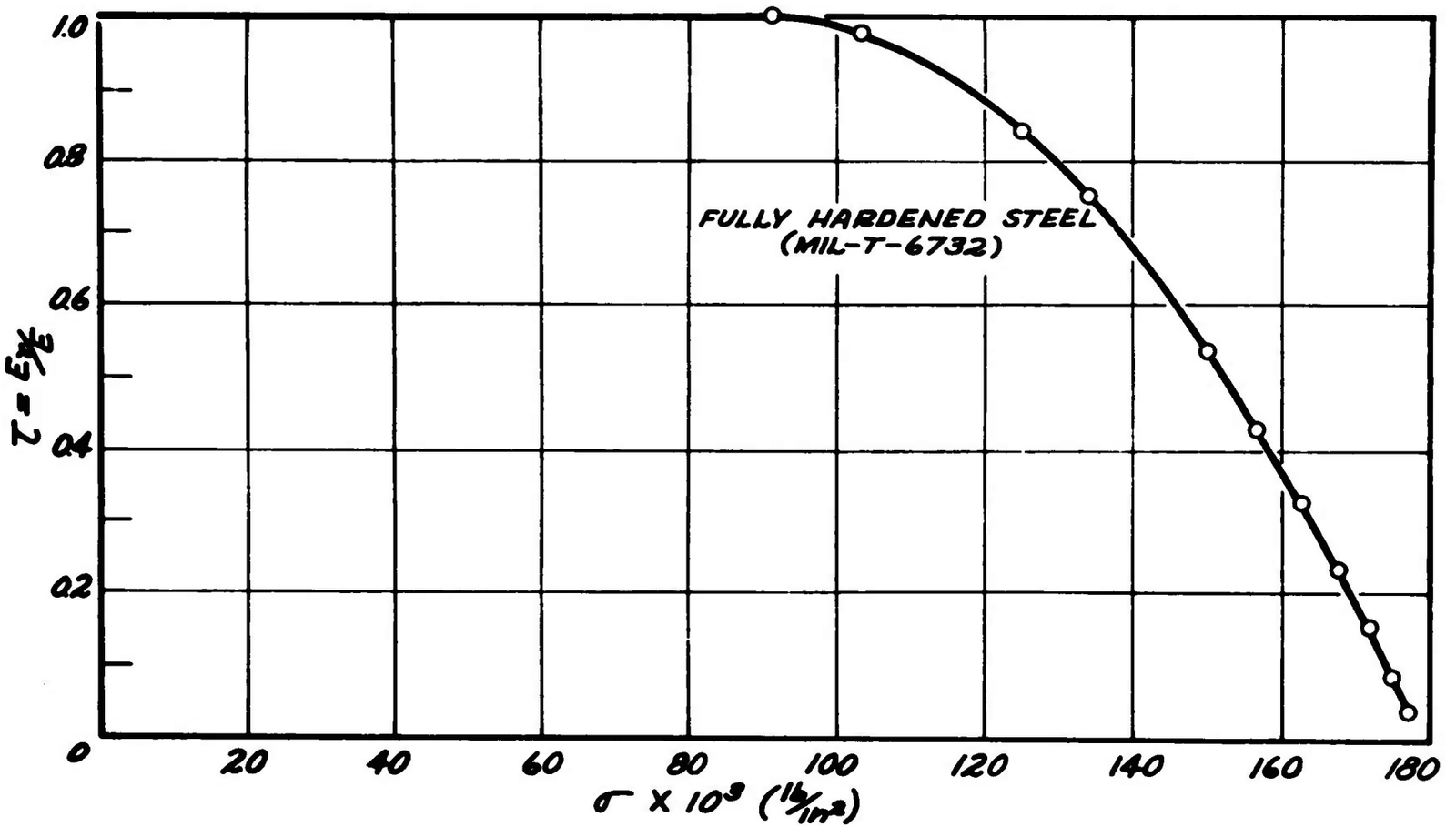

Figure 21. Axial Stress Versus Reduced Modulus Ratio for Fully Hardened Steel (MIL-T-6732).

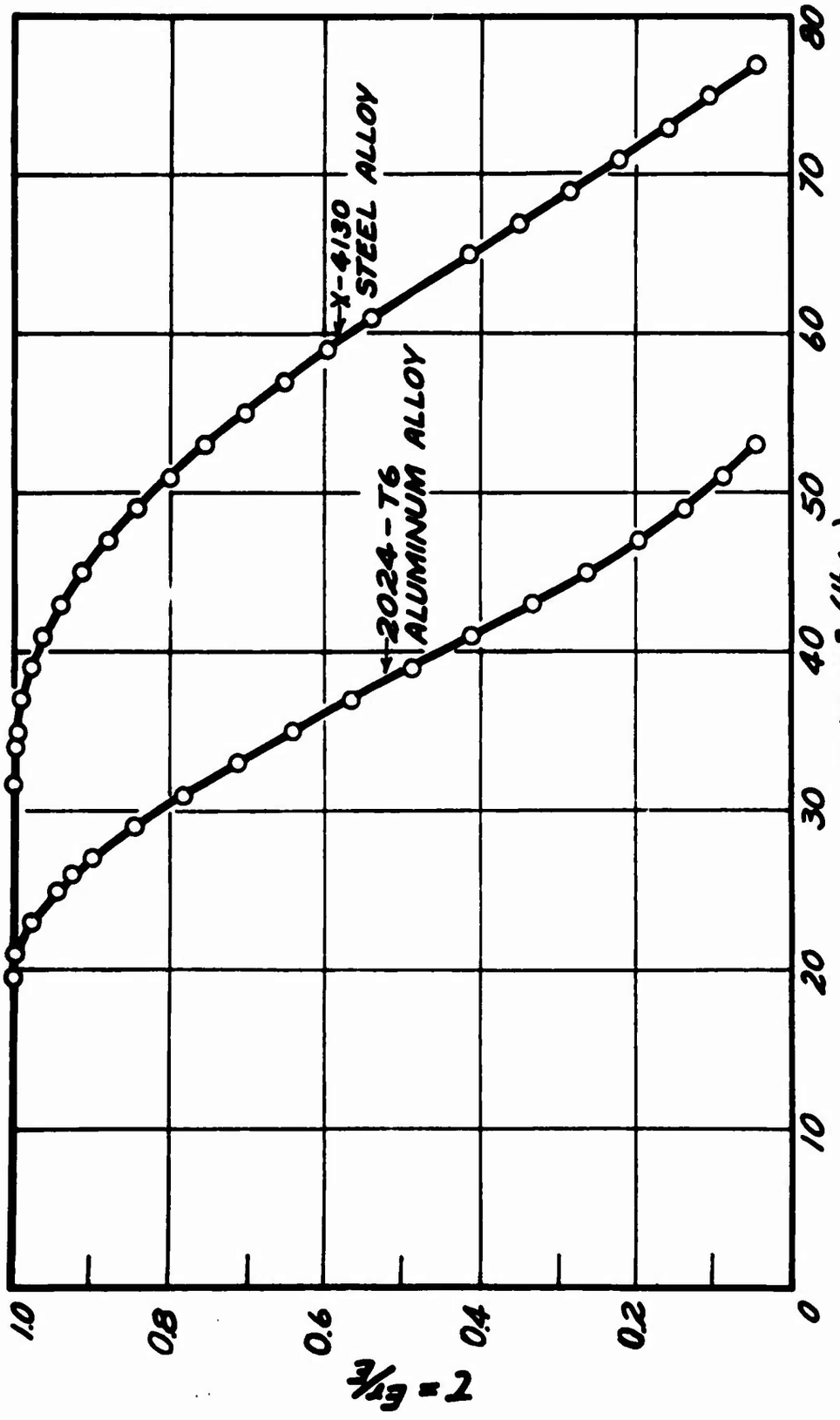

Figure 22. Axial Stress Versus Reduced Modulus Ratio for 2024 Aluminum Alloy and X-4130 Steel Alloy.

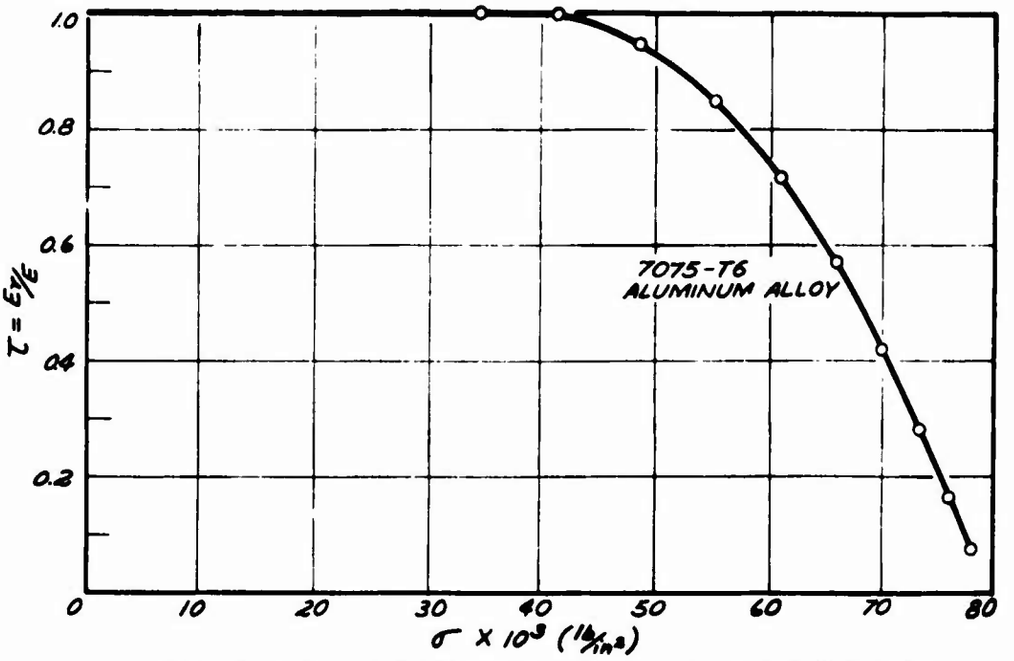

Figure 23. Axial Stress Versus Reduced Modulus Ratio for 7075 Aluminum Alloy.

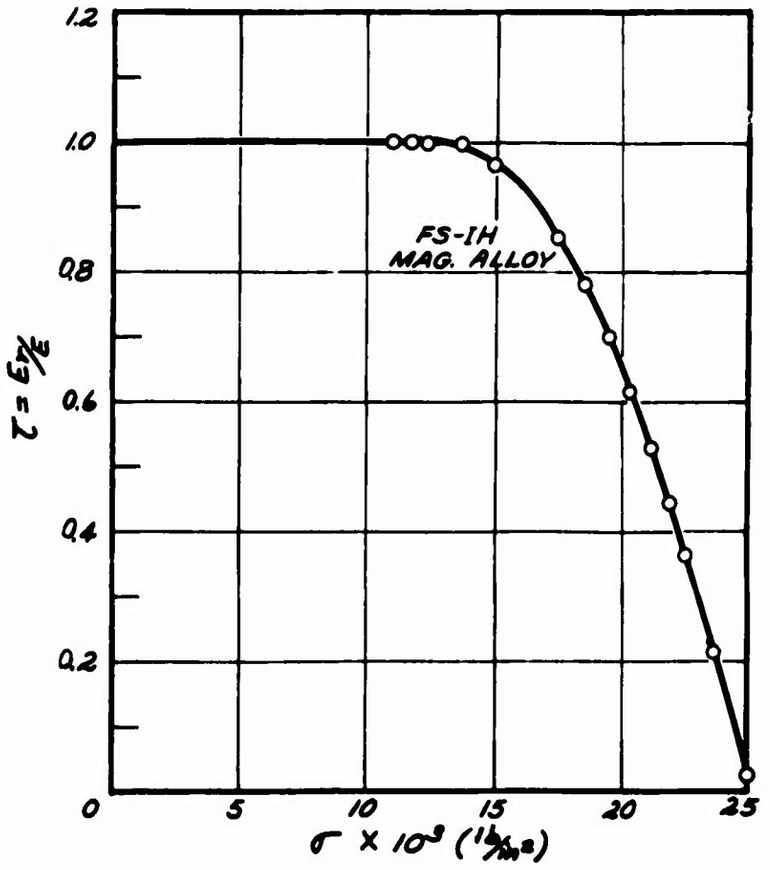

Figure 24.
Axial Stress Versus Reduced Modulus Ratio for FS-1H Magnesium Alloy.

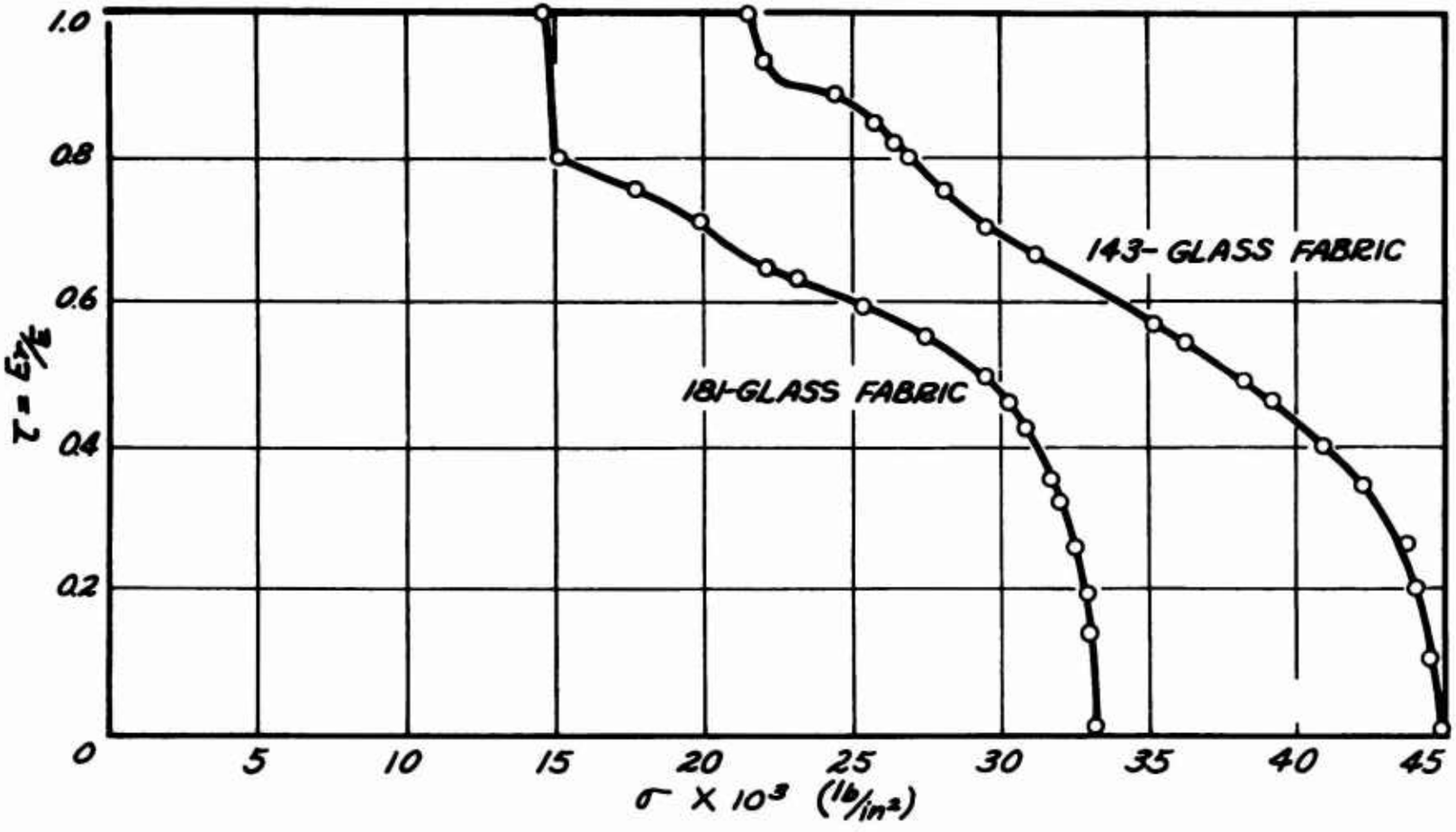

Figure 25. Axial Stress Versus Reduced Modulus Ratio for 181-Glass Fabric and 143-Glass Fabric.

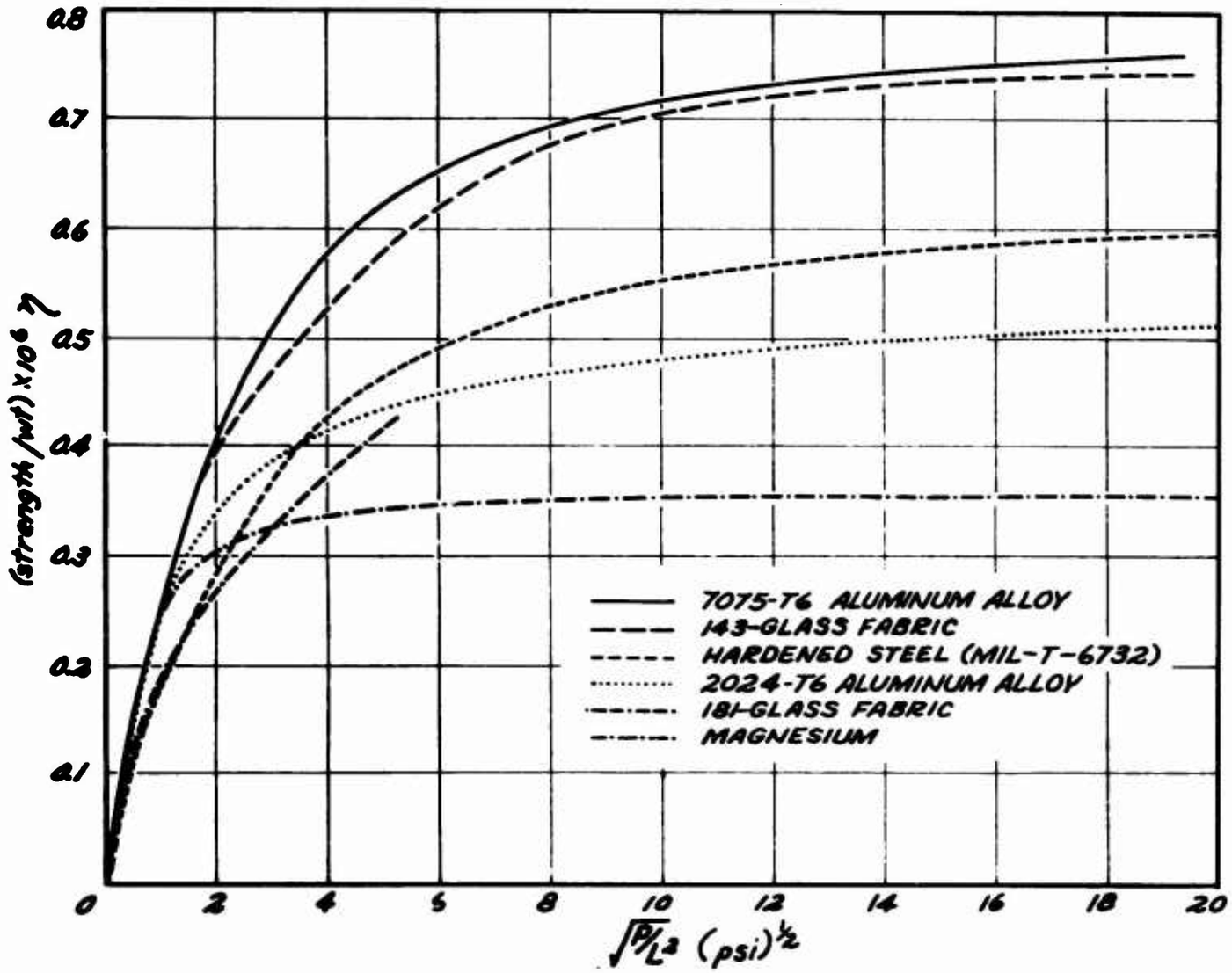

Figure 26. Loading Intensity Versus Efficiency for Circular Column Members.

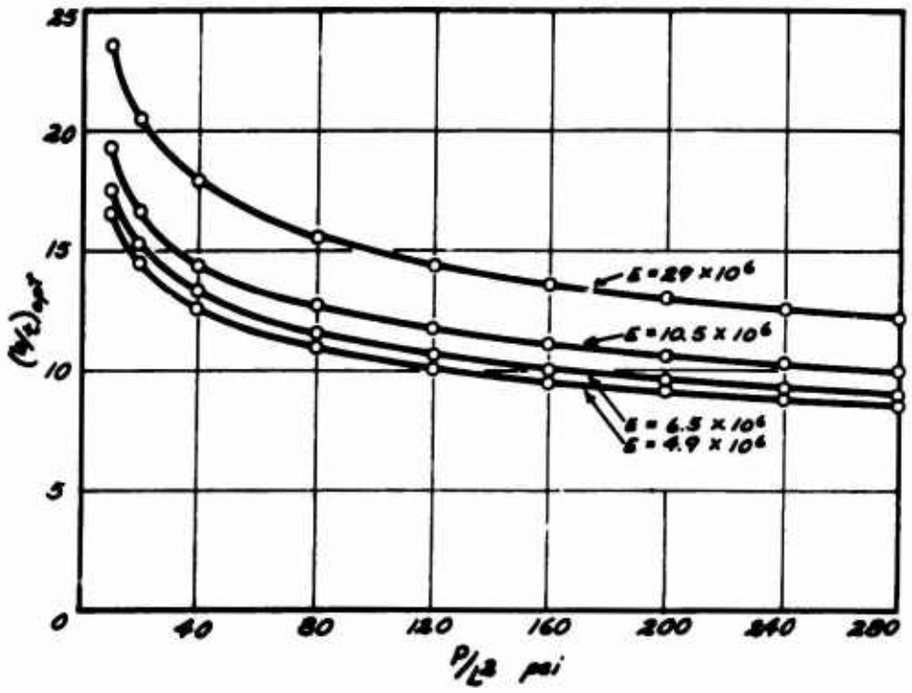

Figure 27a. Optimum Ratio of Applied Load to Column Length Squared Versus Ratio of Semi-Width of Cross Section to Thickness for Rectangular Cross Section Having a Ratio of Semi-Depth of Cross Section to Semi-Width of Cross Section Equal to 0.5.

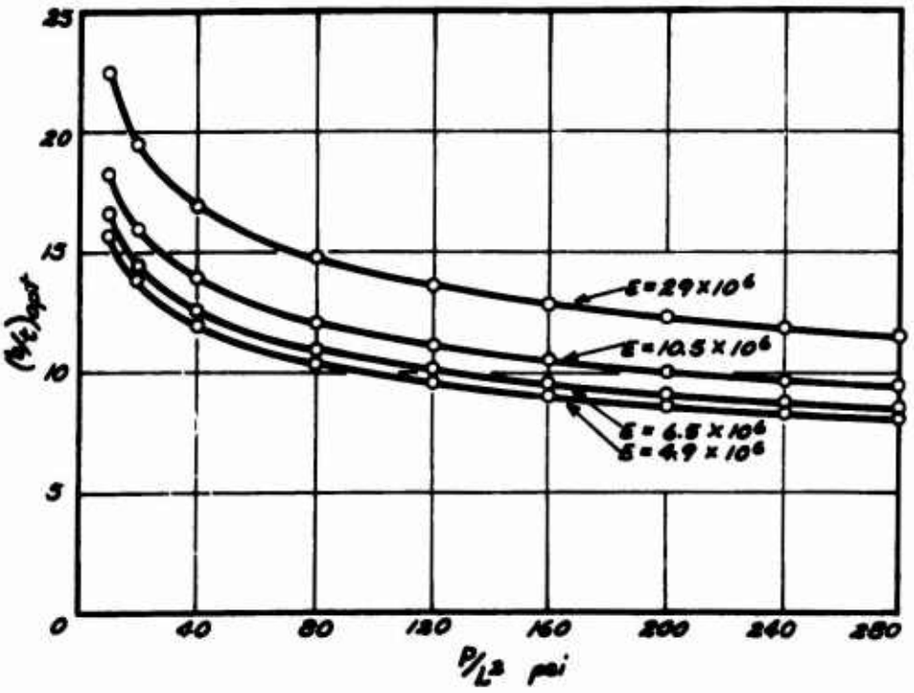

Figure 27b. Optimum Ratio of Applied Load to Column Length Squared Versus Ratio of Semi-Width of Cross Section to Thickness for Rectangular Cross Section Having a Ratio of Semi-Depth of Cross Section to Semi-Width of Cross Section Equal to 0.6.

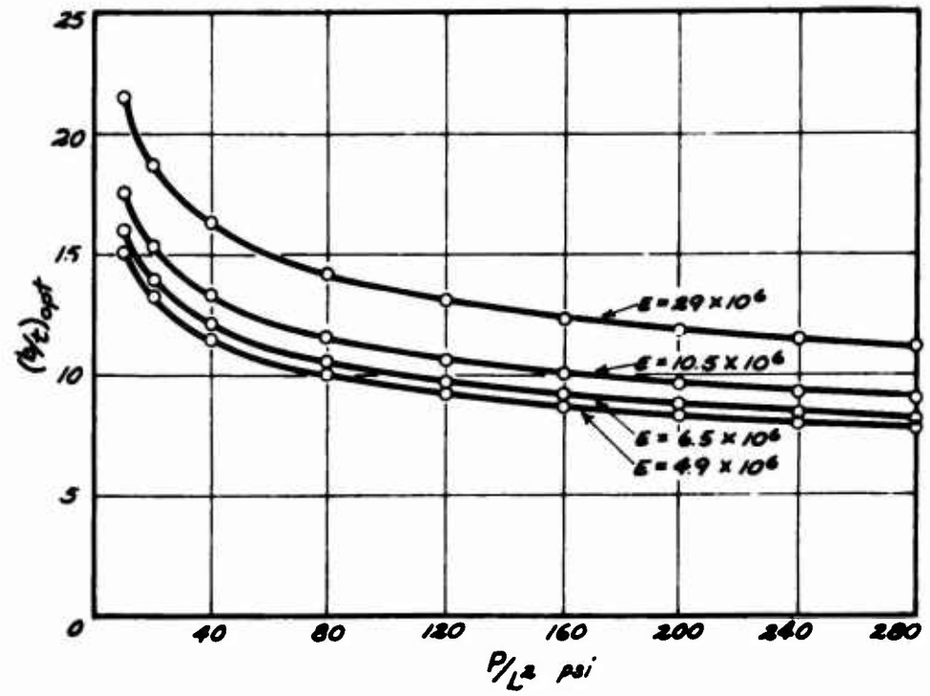

Figure 27c. Optimum Ratio of Applied Load to Column Length Squared Versus Ratio of Semi-Width of Cross Section to Thickness for Rectangular Cross Section Having a Ratio of Semi-Depth of Cross Section to Semi-Width of Cross Section Equal to 0.7.

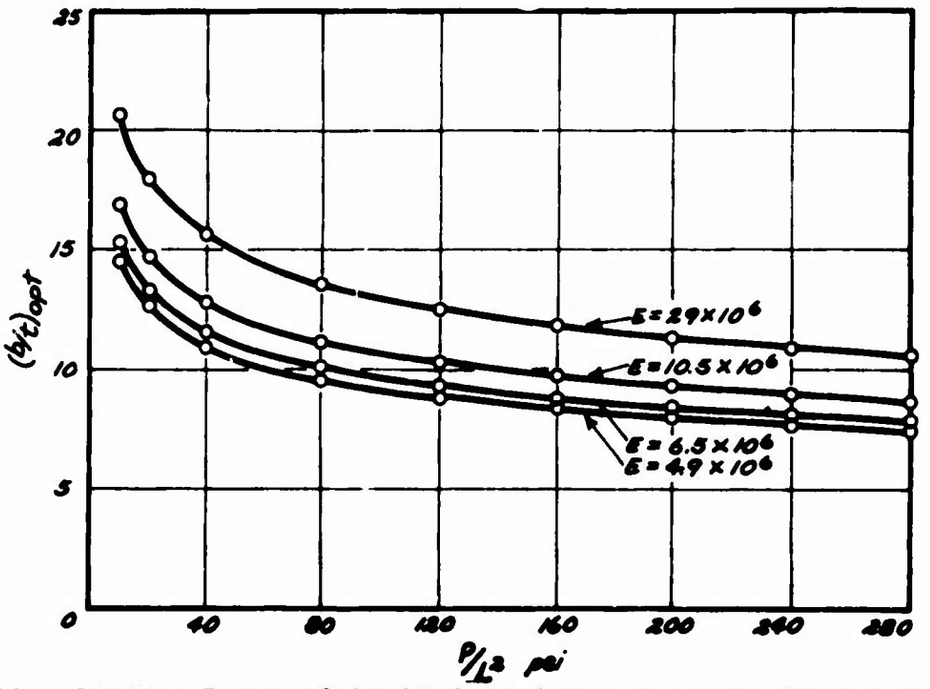

Figure 27d. Optimum Ratio of Applied Load to Column Length Squared Versus Ratio of Semi-Width of Cross Section to Thickness for Rectangular Cross Section Having a Ratio of Semi-Depth of Cross Section to Semi-Width of Cross Section Equal to 0.8.

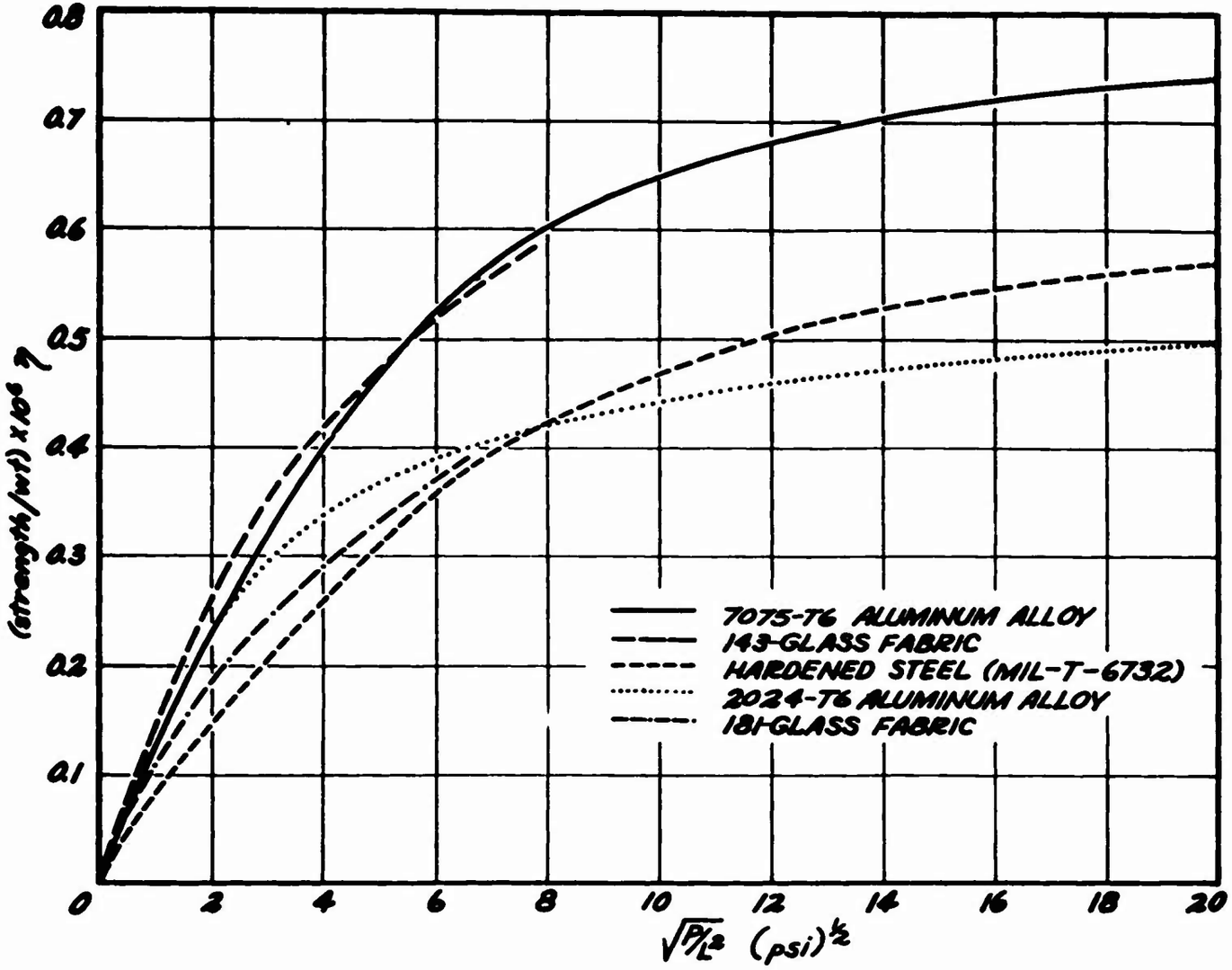

Figure 28. Loading Intensity Versus Efficiency for Rectangular Column Members Having a Ratio of Semi-Depth of Cross Section to Semi-Width of Cross Section Equal to 0.8.

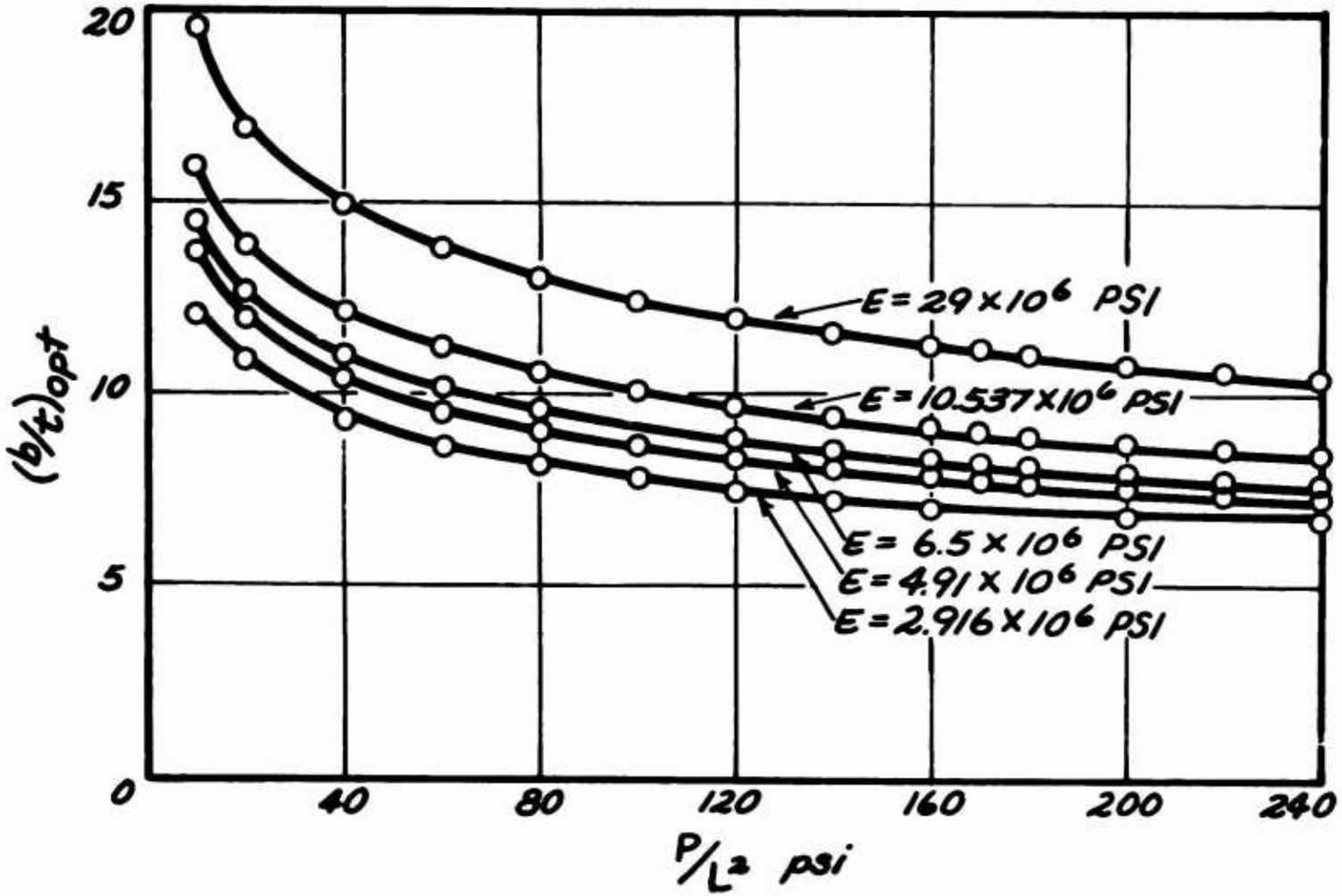

Figure 29. Optimum Ratio of Applied Load to Column Length Squared Versus Ratio of Semi-Width of Cross Section to Thickness for Square Cross Section.

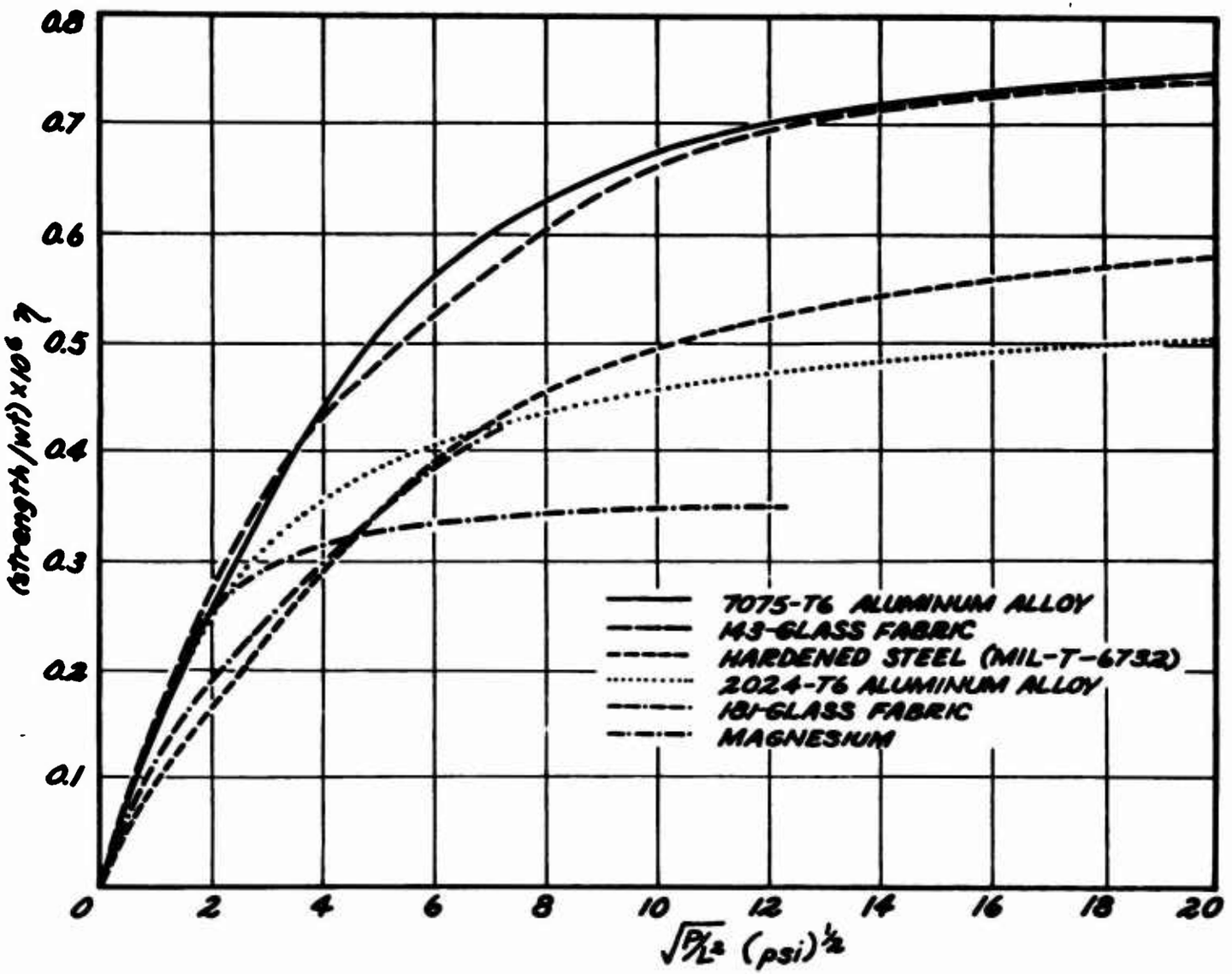

Figure 30. Loading Intensity Versus Efficiency for Square Column Members.

APPENDIX I

RESULTS OF TENSION AND COMPRESSION TESTS OF THE MATERIAL

The properties of the material used, as determined from tension and compression tests, are summarized in the following tables:

TENSILE PROPERTIES OF 181-GLASS FABRIC WITH 4154 POLYESTER RESIN			
Laminate	Angle of Loading	Modulus of Elasticity	Ultimate Strength
181 Fabric	0^{o}	2.54×10^{6} p.s.i.	38000 p.s.i.
	90^{o}	2.38×10^{6} p.s.i.	35200 p.s.i.
	45^{o}	1.46×10^{6} p.s.i.	16985 p.s.i.

COMPRESSIVE PROPERTIES OF 181-GLASS FABRIC WITH 4154 POLYESTER RESIN			
Property	Angle of Loading	Modulus of Elasticity	Ultimate Strength
Average	0^{o}	3.17×10^{6} p.s.i.	33320 p.s.i.
Maximum	0^{o}	3.24×10^{6} p.s.i.	35640 p.s.i.
Minimum	0^{o}	3.10×10^{6} p.s.i.	31000 p.s.i.

APPENDIX II

METHOD OF EVALUATING E_r (2024 ALUMINUM ALLOY)

It is assumed that the pin-ended column strength of 2024 tubes is given by the straight line equation

$$\sigma_{cc} = 58{,}000 - 527\ L/\rho, \tag{4}$$

for values of slenderness ratio L/ρ between 9.5 and 73. Below $L/\rho = 9.5$, it is assumed that the critical stress is 53,000 p.s.i. Above $L/\rho = 73$, the stress is assumed to be given by the Euler formula

$$\sigma_{cr} = \frac{\pi^2 E}{(L/\rho)^2}. \tag{5}$$

The calculations for reduced modulus are made as follows, the results of which are given in Table III.

1. Assume a series of L/ρ
2. Compute σ_{cc} from

$$\sigma_{cc} = 58{,}000 - 527 \quad L/\rho \qquad \text{for } 9.5 < \frac{L}{\rho} < 73$$

$$\sigma_{cc} = \frac{\pi^2 E}{(L/\rho)^2} \qquad \text{for } \frac{L}{\rho} > 73$$

3. Using the computed values of σ_{cc}, compute E_T from

$$E_T = \frac{\sigma_{cc}(L/\rho)^2}{\pi^2}$$

4. Compute τ from $\tau = E_r/E$

In the case of the other materials, reduced modulus (E_T) has been evaluated in the same manner by using appropriate column formulas. The values for each case are given in Tables IV through VIII.

TABLE III
2024-T6 ALUMINUM ALLOY

L/ℓ	σ_{cc}	E_r	E	$\zeta = E_r/E$	$\sqrt{P/L^2}$ Square Section	$\sqrt{P/L^2}$ Circular Section
9.49	53,000	483,600	↑	0.0459	33.68	29.46
13.28	51,000	911,300		0.0865	21.59	17.29
17.08	49,000	1,453,000		0.1379	15.35	11.48
20.87	47,000	2,074,000		0.1968	11.67	8.26
24.67	45,000	2,775,000		0.2633	9.21	6.22
28.46	43,000	3,529,000		0.3349	7.49	4.85
32.26	41,000	4,323,000		0.4103	6.21	3.88
36.05	39,000	5,135,000		0.4874	5.24	3.16
39.85	37,000	5,953,000	10,537,000	0.5650	4.48	2.62
43.64	35,000	6,754,000		0.6409	3.86	2.19
47.44	33,000	7,525,000		0.7141	3.35	1.85
51.23	31,000	8,244,000		0.7823	2.93	1.57
55.03	29,000	8,898,000		0.8444	2.57	1.34
58.82	27,000	9,465,000		0.8982	2.26	1.15
60.72	26,000	9,713,000		0.9215	2.12	1.07
62.62	25,000	9,933,000		0.9426	1.99	0.99
66.41	23,000	10,278,000		0.9754	1.76	0.85
70.21	21,000	10,489,000		0.9954	1.55	0.73
73.00	19,500	10,537,000		1.0000	1.41	0.65
75.00	18,490	10,537,000		1.0000	1.32	0.62
80.00	16,250	10,537,000		1.0000	1.12	0.50

TABLE III - (Contd.)						
L/ℓ	σ_{cc}	E_r	E	$\zeta = E_r/E$	$\sqrt{P/L^2}$ Square Section	$\sqrt{P/L^2}$ Circular Section
85.00	14,390	10,537,000	↓	1.0000	0.96	0.41
90.00	12,840	10,537,000		1.0000	0.83	0.35
95.00	11,520	10,537,000		1.0000	0.73	0.30
100.00	10,400	10,537,000		1.0000	0.64	0.25

TABLE IV 7075-T6 ALUMINUM ALLOY						
L/ℓ	σ_{cc}	E_r	E	$\zeta = E_r/E$	$\sqrt{P/L^2}$ Square Section	$\sqrt{P/L^2}$ Circular Section
10	78,023	790,540	↑	0.0750	40.17	36.41
15	76,115	1,735,220		0.1650	23.83	19.42
20	73,444	2,976,560		0.2820	16.26	12.32
25	70,008	4,433,350		0.4210	11.94	8.49
30	65,810	6,001,120		0.5700	9.15	6.16
35	60,850	7,552,480		0.7170	7.18	4.61
40	55,125	8,936,380		0.8480	5.72	3.51
45	48,635	9,978,900		0.9470	4.56	2.68
50	41,385	10,482,800		0.9950	3.62	2.02
55	34,380	10,537,000	10,537,000	1.0000	2.86	1.53
60	28,887	10,537,000		1.0000	2.30	1.18
65	24,614	10,537,000		1.0000	1.88	0.92
70	21,224	10,537,000		1.0000	1.56	0.74
75	18,490	10,537,000		1.0000	1.32	0.60
80	16,250	10,537,000		1.0000	1.12	0.50
85	14,390	10,537,000		1.0000	0.96	0.41
90	12,840	10,537,000		1.0000	0.83	0.35
95	11,520	10,537,000		1.0000	0.73	0.30
100	10,400	10,537,000	↓	1.0000	0.64	0.25

TABLE V
FULLY HARDENED STEEL ALLOY (MIL-T-6732)

L/ℓ	σ_{cc}	E_r	E	$\tau = E_r/E$	$\sqrt{P/L^2}$ Square Section	$\sqrt{P/L^2}$ Circular Section
8	177,210	1,149,140	↑	0.0400	78.12	72.56
12	174,975	2,552,940		0.0880	46.69	39.40
16	171,845	4,457,360		0.1540	32.22	25.21
20	167,820	6,801,500		0.2350	24.02	17.72
24	162,900	9,507,070		0.3280	18.77	13.20
28	157,090	12,478,370		0.4300	15.13	10.20
32	150,380	15,602,300		0.5380	12.46	8.08
36	142,775	18,748,370		0.6460	10.41	6.51
40	134,280	21,768,690	29×10^6	0.7511	8.79	5.31
44	124,890	24,497,950		0.8450	7.45	4.36
48	114,600	26,753,470		0.9230	6.34	3.58
52	103,420	28,335,150		0.9770	5.38	2.94
56	91,350	29,000,000		1.0000	4.53	2.40
60	79,505	29,000,000		1.0000	3.81	1.95
65	67,745	29,000,000		1.0000	3.12	1.53
70	58,410	29,000,000		1.0000	2.59	1.23
75	50,885	29,000,000		1.0000	2.18	0.9987
80	44,720	29,000,000		1.0000	1.86	0.82
85	39,615	29,000,000		1.0000	1.60	0.69
90	35,335	29,000,000		1.0000	1.38	0.58

TABLE V - (Contd.)						
L/ρ	σ_{cc}	E_r	E	$\tau = E_r/E$	$\sqrt{P/L^2}$ Square Section	$\sqrt{P/L^2}$ Circular Section
95	31,715	29,000,000	↓	1.0000	1.21	0.49
100	38,620	29,000,000	↓	1.0000	1.06	0.42

TABLE VI
MAGNESIUM FS-IH ALLOY

L/ℓ	σ_{cc}	E_r	E	$\tau = E_r/E$	$\sqrt{P/L^2}$ Square Section	$\sqrt{P/L^2}$ Circular Section
8.00	25.04	162,380	↑	0.0250	27.70	24.46
12.00	24.84	362,470		0.0558	16.61	13.24
16.00	24.57	637,210		0.0980	11.52	8.54
20.00	24.21	981,200		0.1510	8.63	6.04
24.00	23.77	1,387,500		0.2135	6.79	4.53
28.00	23.26	1,847,660		0.2843	5.53	3.54
32.00	22.67	2,351,650		0.3618	4.61	2.84
36.00	21.99	2,887,920		0.4443	3.90	2.33
40.00	21.24	3,443,370		0.5297	3.34	1.94
44.00	20.41	4,003,370		0.6159	2.90	1.63
48.00	19.50	4,551,740		0.7003	2.52	1.38
52.00	18.51	5,070,770		0.7801	2.20	1.18
56.00	17.44	5,541,200		0.8525	1.94	1.01
60.00	16.29	5,942,230		0.9142	1.71	0.86
64.00	15.06	6,251,530		0.9618	1.50	0.74
68.00	13.76	6,445,200		0.9916	1.31	0.63
72.00	12.37	6,497,850		0.9997	1.14	0.53
74.00	11.72	6.5×10^6		1.0000	1.07	0.49
76.00	11.11	6.5×10^6		1.0000	1.00	0.45
80.00	10.02	6.5×10^6		1.0000	0.88	0.39
84.00	9.09	6.5×10^6		1.0000	0.78	0.34

6.5×10^6

TABLE VI - (Contd.)

L/ℓ	$\sqrt{\sigma_{cc}}$	E_r	E	$\tau = E_r/E$	$\sqrt{P/L^2}$ Square Section	$\sqrt{P/L^2}$ Circular Section
88.00	8.28	6.5×10^6	↓	1.0000	0.69	0.29
92.00	7.58	6.5×10^6		1.0000	0.62	0.26
96.00	6.96	6.5×10^6		1.0000	0.56	0.23
100.00	6.42	6.5×10^6		1.0000	0.50	

TABLE VII
181-GLASS FABRIC WITH 4154 POLYESTER RESIN

L/ℓ	σ_{cc}	E_r	E	$\tau = E_r/E$	$\sqrt{P/L^2}$ Square Section	$\sqrt{P/L^2}$ Circular Section
10	33,210	337,090	↑	0.1156	27.625	26.409
12	33,050	483,180		0.1657	21.929	20.017
14	32,775	652,310		0.2237	17.991	15.785
16	32,390	841,850		0.2887	15.114	12.806
18	31,730	1,043,635		0.3579	12.877	10.568
20	30,890	1,254,460		0.4302	11.001	8.843
22	29,600	1,454,500		0.4988	9.595	7.424
24	27,550	1,611,090		0.5525	8.229	6.174
26	25,350	1,740,000		0.5967	7.068	5.144
28	23,180	1,845,000		0.6327	6.092	4.304
30	21,200	1,937,100		0.6643	5.285	3.630
32	19,925	2,071,525		0.7104	4.690	3.145
34	18,420	2,161,630		0.7413	4.140	2.707
36	17,000	2,236,900		0.7671	3.666	2.340
38	15,660	2,295,775		0.7873	3.255	2.029
40	14,460	2,349,130		0.8056	2.903	1.769
45	11,860	2.916×10^6		1.000	1.980	1.118
50	9,950	2.916×10^6		1.000	1.590	0.859
55	8,320	2.916×10^6		1.000	1.271	0.657
60	7,000	2.916×10^6		1.000	1.025	0.507

2.916×10^6 p.s.i. ↑

TABLE VII - (Contd.)

L/ℓ	σ_{cc}	E_r	E	$\zeta = E_r/E$	$\sqrt{P/L^2}$ Square Section	$\sqrt{P/L^2}$ Circular Section
65	5,920	2.916×10^6	↓	1.0000	0.831	0.394
70	5,000	2.916×10^6		1.0000	0.673	0.305
75	4,290	2.916×10^6		1.0000	0.555	0.243
80	3,750	2.916×10^6		1.0000	0.470	0.199
85	3,425	2.916×10^6		1.0000	0.419	0.173
90	3,100	2.916×10^6		1.0000	0.317	0.149

TABLE VIII
143-GLASS FABRIC WITH 4154 POLYESTER RESIN

L/ℓ	σ_{cc}	E_r	E	$\tau = E_r/E$	$\sqrt{P/L^2}$ Square Section	$\sqrt{P/L^2}$ Circular Section
9	44,920	368,660	↑	0.0751	35.707	34.108
12	44,742	652,810		0.1329	24.861	22.088
15	44,295	1,009,800		0.2056	18.691	15.683
18	43,348	1,423,050		0.2898	14.683	11.741
21	41,685	1,862,590		0.3793	11.817	9.048
24	39,245	2,290,400		0.4664	9.630	7.078
27	36,252	2,677,710		0.5454	7.909	5.589
30	33,154	3,023,290		0.6157	6.557	4.463
33	30,400	3,354,410		0.6832	5.514	3.625
36	28,200	3,702,990		0.7542	4.719	3.007
39	26,398	4,068,150		0.8285	4.097	2.538
42	24,490	4,377,060		0.8915	3.563	2.147
45	21,595	4,430,875		0.9024	3.022	1.761
50	16,960	4.91×10^6		1.0000	2.095	1.135
55	14,017	4.91×10^6		1.0000	1.651	0.853
60	11,778	4.91×10^6		1.0000	1.328	0.657
65	10,036	4.91×10^6		1.0000	1.087	0.517
70	8,654	4.91×10^6		1.0000	0.903	0.414
75	7,538	4.91×10^6		1.0000	0.760	0.336
80	6,625	4.91×10^6		1.0000	0.647	0.277

4.91×10^6 p.s.i.

TABLE VIII - (Contd.)

L/ρ	σ_{cc}	E_r	E	$\tau = E_r/E$	$\sqrt{P/L^2}$ Square Section	$\sqrt{P/L^2}$ Circular Section
85	5,868	4.91×10^6	↓	1.0000	0.556	0.231
90	5,235	4.91×10^6		1.0000	0.482	0.195

REFERENCES

1. Baskey, R. H., Fiber Reinforcement of Metallic and Nonmetallic Composites, Technical Report 7-924(I), Aeronautical Systems Division, Wright-Patterson Air Force Base, Ohio, February 1962.

2. Boller, Kenneth H., Effect of Thickness on Strength of Epoxy and Phenolic Laminates Reinforced With Glass Fabric, Technical Report 56-522, Wright Air Development Center, Wright-Patterson Air Force Base, Ohio, 1957.

3. Boller, Kenneth H., The Effect of Thickness on Strength of Glass-Fabric-Base Plastic Laminates, Report No. 1831, U. S. Forest Products Laboratory, Madison, Wisconsin, 1953.

4. Boller, Kenneth H., Stress-Rupture Test of a Glass-Fabric-Base Plastic Laminate, Report No. 1839, U. S. Forest Products Laboratory, Madison, Wisconsin, 1953.

5. Cox, H. L. and Smith, H. E., Structures of Minimum Weight, R & M 1923, Aeronautical Research Committee, 1943.

6. Erickson, E. C. O. and Norris, C. B., Tensile Properties of Glass-Fabric Laminates With Laminations Oriented in Any Way, Report No. 1853, U. S. Forest Products Laboratory, Madison, Wisconsin, 1955.

7. Farrar, D. J., "The Design of Compression Structures for Minimum Weight", Journal of the Royal Aeronautical Society, November 1949.

8. Kennedi, R. M. and Harvey, J. M., The Use of Equal Strength Sections in Structural Design, Paper No. 1136, Institute of Engineering and Shipbuilders, 1950.

9. Love, A. E. H., A Treatise on Mathematical Theory of Electricity, Dover Publications, New York, 1944.

10. Nelwin, J. A. and Gahagan, J. M., Tests of Large Timber Columns and Presentation of the Forest Products Laboratory Formulas, Technical Bulletin No. 167, U. S. Forest Products Laboratory, Madison, Wisconsin, February 1930.

11. Peterson, George P., High Modulus Glass-Fiber for Structural Plastics, WADC Technical Report 60-735, Aeronautical System Division, Wright-Patterson Air Force Base, Ohio, 1961.

12. "Reinforced Plastics", Plastics for Flight Vehicles, ANC-17 Bulletin, Part 1, Armed Forces Support Center, Washington, D. C., June 1955.

13. Shanley, F. R., "Principles of Structural Design for Minimum Weight", Aeronautical Science, Volume 16, No. 3, 1949 p. 133.

14. Shanley, F. R., Weight-Strength Analysis of Aircraft Structures, McGraw-Hill Book Company, Inc., New York, 1952.

15. Sonneborn, R. H., Fiberglass Reinforced Plastics, Reinhold Publishing Corporation, New York, 1954.

16. Southwell, R. V., On the Analysis of Experimental Observation in Problems of Elastic Stability, Volume 135, Proceedings of Royal Society of London, 1932, p. 601.

17. Strauss, Erie L., Compression Buckling of Reinforced Plastic Panels, Martin Company, Baltimore, Maryland, September 1958.

18. Timoshenko, S., Theory of Elastic Stability, McGraw-Hill Book Company, Inc., New York, 1936.

19. Werren, Fred and Norris, C. B , Directional Properties of Glass-Fabric-Base Plastic Laminate Panels of Sizes That Do Not Buckle, Report No. 1803 and Supplement A, U. S. Forest Products Laboratory, Madison, Wisconsin, 1949, 1950.

20. Werren, Fred, Effect of Pre-stressing in Tension or Compression on the Mechanical Properties of Two Glass-Fabric-Base Plastic Laminates, Report No. 1811 and Supplement A. U. S. Forest Products Laboratory, Madison, Wisconsin, 1951.

21. Werren, Fred, Effect of Span-Depth Ratio and Thickness on the Mechanical Properties of a Typical Glass-Fabric-Base Plastic Laminate as Determined by Bending Test, Report No. 1807, U. S. Forest Products Laboratory, Madison, Wisconsin, 1949.

22. Werren, Fred, Mechanical Properties of Plastic Laminates, Report No. 1820, Supplements A and B, U. S Forest Products Laboratory, Madison, Wisconsin, 1953, 1955.

23. Wittrick, W. H., A Theoretical Analysis of the Efficiency of Sandwich Construction Under Compressive End Loads, R & M 2016, Aeronautical Research Council, 1945.

24. Youngs, Robert L., Mechanical Properties of Plastic Laminates, Report No. 1820, Supplement B, U. S. Forest Products Laboratory, Madison, Wisconsin, 1956.

UNCLASSIFIED
Security Classification

DOCUMENT CONTROL DATA - R&D

(Security classification of title, body of abstract and indexing annotation must be entered when the overall report is classified)

1. ORIGINATING ACTIVITY (Corporate author)	2a. REPORT SECURITY CLASSIFICATION
Mississippi State University Aerophysics Department State College, Mississippi	Unclassified 2b. GROUP

3. REPORT TITLE

A PRELIMINARY STUDY TO DETERMINE THE FEASIBILITY OF REINFORCED PLASTIC COLUMN MEMBERS FOR AIRCRAFT STRUCTURES

4. DESCRIPTIVE NOTES (Type of report and inclusive dates)

5. AUTHOR(S) (Last name, first name, initial)

Dev R. Bhandari

6. REPORT DATE	7a. TOTAL NO. OF PAGES	7b. NO. OF REFS
December 1965	62	24

8a. CONTRACT OR GRANT NO.	9a. ORIGINATOR'S REPORT NUMBER(S)
DA 44-177-AMC-892(T) b. PROJECT NO. Task 1P125901A14203 c. d.	USAAVLABS Technical Report 65-76 9b. OTHER REPORT NO(S) (Any other numbers that may be assigned this report) Aerophysics Research Report No. 60

10. AVAILABILITY/LIMITATION NOTICES

Distribution of this document is unlimited.

11. SUPPLEMENTARY NOTES	12. SPONSORING MILITARY ACTIVITY
	U. S. Army Aviation Materiel Laboratories Fort Eustis, Virginia

13. ABSTRACT

Empirical formulas for predicting the critical buckling stress of fiber glass reinforced plastic columns have been obtained. On the basis of these buckling formulas, structural efficiency of fiber glass reinforced plastic column members of different cross sections is compared with other commonly used structural alloys. The efficiency parameter used for comparison is derived on the minimum weight design considerations.

DD FORM 1 JAN 64 1473

UNCLASSIFIED
Security Classification

14. KEY WORDS	LINK A		LINK B		LINK C	
	ROLE	WT	ROLE	WT	ROLE	WT

INSTRUCTIONS

1. **ORIGINATING ACTIVITY:** Enter the name and address of the contractor, subcontractor, grantee, Department of Defense activity or other organization *(corporate author)* issuing the report.

2a. **REPORT SECURITY CLASSIFICATION:** Enter the overall security classification of the report. Indicate whether "Restricted Data" is included. Marking is to be in accordance with appropriate security regulations.

2b. **GROUP:** Automatic downgrading is specified in DoD Directive 5200.10 and Armed Forces Industrial Manual. Enter the group number. Also, when applicable, show that optional markings have been used for Group 3 and Group 4 as authorized.

3. **REPORT TITLE:** Enter the complete report title in all capital letters. Titles in all cases should be unclassified. If a meaningful title cannot be selected without classification, show title classification in all capitals in parenthesis immediately following the title.

4. **DESCRIPTIVE NOTES:** If appropriate, enter the type of report, e.g., interim, progress, summary, annual, or final. Give the inclusive dates when a specific reporting period is covered.

5. **AUTHOR(S):** Enter the name(s) of author(s) as shown on or in the report. Enter last name, first name, middle initial. If military, show rank and branch of service. The name of the principal author is an absolute minimum requirement.

6. **REPORT DATE:** Enter the date of the report as day, month, year; or month, year. If more than one date appears on the report, use date of publication.

7a. **TOTAL NUMBER OF PAGES:** The total page count should follow normal pagination procedures, i.e., enter the number of pages containing information.

7b. **NUMBER OF REFERENCES:** Enter the total number of references cited in the report.

8a. **CONTRACT OR GRANT NUMBER:** If appropriate, enter the applicable number of the contract or grant under which the report was written.

8b, 8c, & 8d. **PROJECT NUMBER:** Enter the appropriate military department identification, such as project number, subproject number, system numbers, task number, etc.

9a. **ORIGINATOR'S REPORT NUMBER(S):** Enter the official report number by which the document will be identified and controlled by the originating activity. This number must be unique to this report.

9b. **OTHER REPORT NUMBER(S):** If the report has been assigned any other report numbers *(either by the originator or by the sponsor)*, also enter this number(s).

10. **AVAILABILITY/LIMITATION NOTICES:** Enter any limitations on further dissemination of the report, other than those imposed by security classification, using standard statements such as:

(1) "Qualified requesters may obtain copies of this report from DDC."

(2) "Foreign announcement and dissemination of this report by DDC is not authorized."

(3) "U. S. Government agencies may obtain copies of this report directly from DDC. Other qualified DDC users shall request through _____."

(4) "U. S. military agencies may obtain copies of this report directly from DDC. Other qualified users shall request through _____."

(5) "All distribution of this report is controlled. Qualified DDC users shall request through _____."

If the report has been furnished to the Office of Technical Services, Department of Commerce, for sale to the public, indicate this fact and enter the price, if known.

11. **SUPPLEMENTARY NOTES:** Use for additional explanatory notes.

12. **SPONSORING MILITARY ACTIVITY:** Enter the name of the departmental project office or laboratory sponsoring *(paying for)* the research and development. Include address.

13. **ABSTRACT:** Enter an abstract giving a brief and factual summary of the document indicative of the report, even though it may also appear elsewhere in the body of the technical report. If additional space is required, a continuation sheet shall be attached.

It is highly desirable that the abstract of classified reports be unclassified. Each paragraph of the abstract shall end with an indication of the military security classification of the information in the paragraph, represented as *(TS), (S), (C), or (U).*

There is no limitation on the length of the abstract. However, the suggested length is from 150 to 225 words.

14. **KEY WORDS:** Key words are technically meaningful terms or short phrases that characterize a report and may be used as index entries for cataloging the report. Key words must be selected so that no security classification is required. Idenfiers, such as equipment model designation, trade name, military project code name, geographic location, may be used as key words but will be followed by an indication of technical context. The assignment of links, rules, and weights is optional.